Springer

Dear Author,

Here are the proofs of your article.

- You can submit your corrections **online**, via **e-mail** or by **fax**.
- For **online** submission please insert your corrections in the online correction form. Always indicate the line number to which the correction refers.
- You can also insert your corrections in the proof PDF and **email** the annotated PDF.
- For fax submission, please ensure that your corrections are clearly legible. Use a fine black pen and write the correction in the margin, not too close to the edge of the page.
- Remember to note the **journal title**, **article number**, and **your name** when sending your response via e-mail or fax.
- **Check** the metadata sheet to make sure that the header information, especially author names and the corresponding affiliations are correctly shown.
- **Check** the questions that may have arisen during copy editing and insert your answers/ corrections.
- **Check** that the text is complete and that all figures, tables and their legends are included. Also check the accuracy of special characters, equations, and electronic supplementary material if applicable. If necessary refer to the *Edited manuscript*.
- The publication of inaccurate data such as dosages and units can have serious consequences. Please take particular care that all such details are correct.
- Please **do not** make changes that involve only matters of style. We have generally introduced forms that follow the journal's style.
  Substantial changes in content, e.g., new results, corrected values, title and authorship are not allowed without the approval of the responsible editor. In such a case, please contact the Editorial Office and return his/her consent together with the proof.
- If we do not receive your corrections **within 48 hours**, we will send you a reminder.
- Your article will be published **Online First** approximately one week after receipt of your corrected proofs. This is the **official first publication** citable with the DOI. **Further changes are, therefore, not possible.**
- The **printed version** will follow in a forthcoming issue.

Please note

After online publication, subscribers (personal/institutional) to this journal will have access to the complete article via the DOI using the URL: http://dx.doi.org/[DOI].
If you would like to know when your article has been published online, take advantage of our free alert service. For registration and further information go to: http://www.link.springer.com.

Due to the electronic nature of the procedure, the manuscript and the original figures will only be returned to you on special request. When you return your corrections, please inform us if you would like to have these documents returned.

Metadata of the article that will be visualized in OnlineFirst

ArticleTitle	An afocal telescope configuration for the ESA ARIEL mission	
Article Sub-Title		
Article CopyRight	CEAS (This will be the copyright line in the final PDF)	
Journal Name	CEAS Space Journal	
Corresponding Author	Family Name	**Deppo**
	Particle	**Da**
	Given Name	**Vania**
	Suffix	
	Division	
	Organization	CNR-IFN Padova
	Address	Via Trasea 7, 35131, Padua, Italy
	Division	
	Organization	INAF-Osservatorio Astronomico di Padova
	Address	Vicolo dell'Osservatorio 5, 35122, Padua, Italy
	Phone	049-9815639
	Fax	
	Email	vania.dadeppo@ifn.cnr.it
	URL	
	ORCID	http://orcid.org/0000-0001-6273-8738
Author	Family Name	**Focardi**
	Particle	
	Given Name	**Mauro**
	Suffix	
	Division	
	Organization	INAF-Osservatorio Astrofisico di Arcetri
	Address	Largo E. Fermi 5, 50125, Florence, Italy
	Phone	
	Fax	
	Email	
	URL	
	ORCID	
Author	Family Name	**Middleton**
	Particle	
	Given Name	**Kevin**
	Suffix	
	Division	
	Organization	RAL Space-STFC Rutherford Appleton Laboratory
	Address	Harwell Campus, Didcot, OX11 0QX, UK
	Phone	

	Fax	
	Email	
	URL	
	ORCID	
Author	Family Name	**Morgante**
	Particle	
	Given Name	**Gianluca**
	Suffix	
	Division	
	Organization	INAF-IASF Bologna
	Address	Area della Ricerca, Via Piero Gobetti 101, 40129, Bologna, Italy
	Phone	
	Fax	
	Email	
	URL	
	ORCID	
Author	Family Name	**Pascale**
	Particle	
	Given Name	**Enzo**
	Suffix	
	Division	
	Organization	Dip. di Fisica-Università degli Studi di Roma “La Sapienza”
	Address	Piazzale Aldo Moro 2, 00185, Rome, Italy
	Division	School of Physics and Astronomy
	Organization	Cardiff University
	Address	5 The Parade, Cardiff, NSW, CF24 3AA, UK
	Phone	
	Fax	
	Email	
	URL	
	ORCID	
Author	Family Name	**Grella**
	Particle	
	Given Name	**Samuele**
	Suffix	
	Division	
	Organization	Leonardo S.p.A
	Address	Via delle Officine Galileo 1, 50013, Florence, Campi Bisenzio, Italy
	Phone	
	Fax	
	Email	
	URL	
	ORCID	
Author	Family Name	**Pace**
	Particle	

	Given Name	**Emanuele**
	Suffix	
	Division	
	Organization	Dip. di Fisica ed Astronomia-Università degli Studi di Firenze
	Address	Largo E. Fermi 2, 50125, Florence, Italy
	Phone	
	Fax	
	Email	
	URL	
	ORCID	
Author	Family Name	**Claudi**
	Particle	
	Given Name	**Riccardo**
	Suffix	
	Division	
	Organization	INAF-Osservatorio Astronomico di Padova
	Address	Vicolo dell'Osservatorio 5, 35122, Padua, Italy
	Phone	
	Fax	
	Email	
	URL	
	ORCID	
Author	Family Name	**Amiaux**
	Particle	
	Given Name	**Jerome**
	Suffix	
	Division	Laboratoire Léon Brillouin
	Organization	UMR12, CEA-CNRS
	Address	91191, Saclay, Gif sur Yvette, France
	Phone	
	Fax	
	Email	
	URL	
	ORCID	
Author	Family Name	**Ferrer**
	Particle	
	Given Name	**Josep Colomé**
	Suffix	
	Division	
	Organization	Institut de Ciències de l'Espai, (CSIC-IEEC)
	Address	Campus UAB, 08193, Bellaterra, Barcelona, Spain
	Phone	
	Fax	
	Email	
	URL	

	ORCID	
Author	Family Name	**Hunt**
	Particle	
	Given Name	**Thomas**
	Suffix	
	Division	Mullard Space Science Laboratory
	Organization	Holmbury St. Mary
	Address	Dorking, Surrey, RH5 6NT, UK
	Phone	
	Fax	
	Email	
	URL	
	ORCID	
Author	Family Name	**Rataj**
	Particle	
	Given Name	**Miroslaw**
	Suffix	
	Division	Space Research Centre
	Organization	Polish Academy of Sciences
	Address	Bartycka 18A, 00-716, Warsaw, Poland
	Phone	
	Fax	
	Email	
	URL	
	ORCID	
Author	Family Name	**Sierra-Roig**
	Particle	
	Given Name	**Carles**
	Suffix	
	Division	
	Organization	Institut de Ciències de l'Espai, (CSIC-IEEC)
	Address	Campus UAB, 08193, Bellaterra, Barcelona, Spain
	Phone	
	Fax	
	Email	
	URL	
	ORCID	
Author	Family Name	**Veltroni**
	Particle	
	Given Name	**Iacopo Ficai**
	Suffix	
	Division	
	Organization	Leonardo S.p.A
	Address	Via delle Officine Galileo 1, 50013, Florence, Campi Bisenzio, Italy
	Phone	

	Fax	
	Email	
	URL	
	ORCID	
Author	Family Name	**Eccleston**
	Particle	
	Given Name	**Paul**
	Suffix	
	Division	
	Organization	RAL Space-STFC Rutherford Appleton Laboratory
	Address	Harwell Campus, Didcot, OX11 0QX, UK
	Phone	
	Fax	
	Email	
	URL	
	ORCID	
Author	Family Name	**Micela**
	Particle	
	Given Name	**Giuseppina**
	Suffix	
	Division	
	Organization	INAF-Osservatorio Astronomico di Palermo
	Address	Piazza del Parlamento 1, 90134, Palermo, Italy
	Phone	
	Fax	
	Email	
	URL	
	ORCID	
Author	Family Name	**Tinetti**
	Particle	
	Given Name	**Giovanna**
	Suffix	
	Division	Department of Physics and Astronomy
	Organization	University College London
	Address	Gower Street, London, WC1E 6BT, UK
	Phone	
	Fax	
	Email	
	URL	
	ORCID	

Schedule	Received	29 May 2017
	Revised	26 September 2017
	Accepted	6 October 2017

Abstract — Atmospheric Remote-Sensing Infrared Exoplanet Large Survey (ARIEL) is a candidate as an M4 ESA mission to launch in 2026. During its 3.5 years of scientific operations, ARIEL will observe

	spectroscopically in the infrared (IR) a large population of known transiting planets in the neighbourhood of the solar system. ARIEL aims to give a breakthrough in the observation of exoplanet atmospheres and understanding of the physics and chemistry of these far-away worlds. ARIEL is based on a 1 m class telescope feeding a collimated beam into two separate instrument modules: a spectrometer module covering the waveband between 1.95 and 7.8 μm and a combined fine guidance system/visible photometer/NIR spectrometer. The telescope configuration is a classic Cassegrain layout used with an eccentric pupil and coupled to a tertiary off-axis paraboloidal mirror. To constrain the thermo-mechanically induced optical aberrations, the primary mirror (M1) temperature will be monitored and finely tuned using an active thermal control system based on thermistors and heaters. They will be switched on and off to maintain the M1 temperature within ± 1 K by the telescope control unit (TCU). The TCU is a payload electronics subsystem also responsible for the thermal control of the spectrometer module detectors as well as the secondary mirror mechanism and IR calibration source management. The TCU, being a slave subsystem of the instrument control unit, will collect the housekeeping data from the monitored subsystems and will forward them to the master unit. The latter will run the application software, devoted to the main spectrometer management and to the scientific data on-board processing.
Keywords (separated by '-')	Space instrumentation - Telescope - Optical design - Exoplanetary science - Active thermal control - ICU
Footnote Information	This paper is based on a presentation at the International Conference on Space Optics (ICSO), 18–21 October, 2016, Biarritz, France.

CEAS Space J
DOI 10.1007/s12567-017-0175-3

ORIGINAL PAPER

An afocal telescope configuration for the ESA ARIEL mission

Vania Da Deppo[1,2] · Mauro Focardi[3] · Kevin Middleton[4] · Gianluca Morgante[5] · Enzo Pascale[6,7] · Samuele Grella[8] · Emanuele Pace[9] · Riccardo Claudi[2] · Jerome Amiaux[10] · Josep Colomé Ferrer[11] · Thomas Hunt[12] · Miroslaw Rataj[13] · Carles Sierra-Roig[11] · Iacopo Ficai Veltroni[8] · Paul Eccleston[4] · Giuseppina Micela[14] · Giovanna Tinetti[15]

Received: 29 May 2017 / Revised: 26 September 2017 / Accepted: 6 October 2017

Abstract Atmospheric Remote-Sensing Infrared Exoplanet Large Survey (ARIEL) is a candidate as an M4 ESA mission to launch in 2026. During its 3.5 years of scientific operations, ARIEL will observe spectroscopically in the infrared (IR) a large population of known transiting planets in the neighbourhood of the solar system. ARIEL aims to give a breakthrough in the observation of exoplanet atmospheres and understanding of the physics and chemistry of these far-away worlds. ARIEL is based on a 1 m class telescope feeding a collimated beam into two separate instrument modules: a spectrometer module covering the waveband between 1.95 and 7.8 μm and a combined fine guidance system/visible photometer/NIR spectrometer. The telescope configuration is a classic Cassegrain layout used with an eccentric pupil and coupled to a tertiary off-axis paraboloidal mirror. To constrain the thermo-mechanically induced optical aberrations, the primary mirror (M1) temperature will be monitored and finely tuned using an active thermal control system based on thermistors and heaters. They will be switched on and off to maintain the M1 temperature within ± 1 K by the telescope control unit (TCU). The TCU is a payload electronics subsystem also responsible for the thermal control of the spectrometer module detectors as well as the secondary mirror mechanism and IR calibration source management. The TCU, being a slave subsystem of the instrument control unit, will collect the housekeeping data from the monitored subsystems and will forward them to the master unit. The latter will run the application

This paper is based on a presentation at the International Conference on Space Optics (ICSO), 18–21 October, 2016, Biarritz, France.

✉ Vania Da Deppo
vania.dadeppo@ifn.cnr.it

[1] CNR-IFN Padova, Via Trasea 7, 35131 Padua, Italy
[2] INAF-Osservatorio Astronomico di Padova, Vicolo dell'Osservatorio 5, 35122 Padua, Italy
[3] INAF-Osservatorio Astrofisico di Arcetri, Largo E. Fermi 5, 50125 Florence, Italy
[4] RAL Space-STFC Rutherford Appleton Laboratory, Harwell Campus, Didcot OX11 0QX, UK
[5] INAF-IASF Bologna, Area della Ricerca, Via Piero Gobetti 101, 40129 Bologna, Italy
[6] Dip. di Fisica-Università degli Studi di Roma "La Sapienza", Piazzale Aldo Moro 2, 00185 Rome, Italy
[7] School of Physics and Astronomy, Cardiff University, 5 The Parade, Cardiff, NSW CF24 3AA, UK
[8] Leonardo S.p.A, Via delle Officine Galileo 1, 50013 Florence, Campi Bisenzio, Italy
[9] Dip. di Fisica ed Astronomia-Università degli Studi di Firenze, Largo E. Fermi 2, 50125 Florence, Italy
[10] Laboratoire Léon Brillouin, UMR12, CEA-CNRS, 91191 Saclay, Gif sur Yvette, France
[11] Institut de Ciències de l'Espai, (CSIC-IEEC), Campus UAB, 08193 Bellaterra, Barcelona, Spain
[12] Mullard Space Science Laboratory, Holmbury St. Mary, Dorking, Surrey RH5 6NT, UK
[13] Space Research Centre, Polish Academy of Sciences, Bartycka 18A, 00-716 Warsaw, Poland
[14] INAF-Osservatorio Astronomico di Palermo, Piazza del Parlamento 1, 90134 Palermo, Italy
[15] Department of Physics and Astronomy, University College London, Gower Street, London WC1E 6BT, UK

software, devoted to the main spectrometer management and to the scientific data on-board processing.

Keywords Space instrumentation · Telescope · Optical design · Exoplanetary science · Active thermal control · ICU

1 Introduction

ARIEL is one of the M4 proposed missions in the framework of the ESA Cosmic Vision program [1]. The ARIEL mission will address the fundamental questions on what exoplanets are made of and how planetary systems form and evolve by investigating the atmospheres of many hundreds of diverse known exoplanets orbiting different types of nearby stars [2].

About three thousand exoplanets have now been discovered; Gaia [3], Kepler [4], and K2 [5], together with other current ground and space-based surveys, will continue to increase the known exoplanet list. However, at present, very little is known about the nature of these exoplanets. During its 3.5-year scientific mission lifetime in L2 orbit, the ARIEL mission aims to measure the atmospheric composition and structure of a large and well-defined selected sample of exoplanets (~ 1000). It will use transit spectroscopy in the 1.25–7.8 μm spectral range and multiple narrow-band photometry in the optical.

For its ambitious scientific program, ARIEL is designed as a dedicated survey mission for transit and eclipse spectroscopy, whereby the signal from the star and planet is differentiated using knowledge of the planetary ephemerides, transit, and eclipse and phase-curve spectroscopy methods allow to measure atmospheric signals from the planet at levels of 10–100 part per million (ppm) relative to the star and, given the bright nature of the targets, also allow more sophisticated techniques, such as eclipse mapping, to give a deeper insight into the nature of the atmosphere.

This mission will allow the exploration and sounding of the nature of the exoplanet atmospheres, to collect information about the planet interiors and to study the key factors affecting the formation and evolution of planetary systems [6].

Some simulations of the ARIEL performance in conducting exoplanet surveys have been performed. For this purpose, three elements have been taken into account: a conservative estimate of the mission performance, a full model of all the possible significant noise sources present in the measurements, and a list of the potential ARIEL targets that incorporate the latest available exoplanet statistics. The conclusion is that ARIEL will be able to observe 500–1000 exoplanets, depending on the details of the adopted survey strategy, and the feasibility of the main science objectives is confirmed.

ARIEL will be highly complementary to other international facilities (such as TESS [7], to be launched in 2018) and will benefit from other ESA exoplanet missions such as CHEOPS [8] and PLATO [9], which will help to provide an optimized target list prior to launch.

At the beginning of this paper, the ARIEL mission science objectives and requirements will be presented (Sect. 2). Then, the description of the spacecraft and the science payload will follow (Sect. 3). After that, the discussion of the requirements and the design of the telescope will be given (Sect. 4). The solution adopted for cooling the payload and the results of the thermal analysis will be presented in Sect. 5; while the design details of the electronic units (ICU and TCU) controlling the instrument will be analysed in the last part (Sect. 6).

2 The ARIEL mission science

2.1 ARIEL observation strategy and science requirements

Depending on their mass, the exoplanets have been so far divided into three categories: rocky/icy planets ($< 5\ M_{\mathrm{Earth}}$), gas rich planets ($> 15\ M_{\mathrm{Earth}}$), and transitional planets (5–15 M_{Earth}). The ARIEL selected exoplanet target sample will ensure to observe a statistically significant population for each of these three classes.

Different observation techniques will be used to gain information on different parts of the exoplanet atmospheres. Terminator regions will be studied with transit spectroscopy, day-side hemisphere via planetary eclipse spectroscopy and unilluminated night-side hemisphere using phase variation. In addition, the eclipse mapping method can be used to spatially resolve the day-side hemisphere and the repeated observation of a number of key planets in both transit and eclipse mode (i.e., time series of narrow spectral bands) will allow the monitoring of global meteorological variations and to probe cloud distribution and patchiness [6].

The ARIEL observation strategy is divided into three tiers. The first one is a "reconnaissance survey" during which the selected 1000 exoplanet sample will be observed with low spectral resolution and SNR. This will allow to classify the exoplanet atmospheres and select the good candidates for further studies. The second phase is a "deep survey", i.e., high spectral resolution observation in the Vis–IR of an exoplanet sub-sample, to determine the atmospheric components, chemical abundances, and thermal structure. The last tier is "benchmark planets"; the very best planets, which means those very interesting from a scientific point of view, will be re-observed multiple times with all the techniques for a detailed knowledge of the planetary chemistry and dynamics, weather, and spatial and temporal variabilities.

Journal : Large 12567 | Article No : 175 | Pages : 20 | MS Code : CEAS-D-17-00051 | Dispatch : 26-10-2017

The key science performance parameters that will drive the specification of the ARIEL mission have been identified by the Science Study Team (SST) [10]. These requirements have been derived starting from the science objective, and they include the wavelength coverage, spectral resolving power, signal-to-noise ratio and noise requirements, photometric stability, sky visibility/source accessibility, temporal resolution, limiting targets, calibration, and zodiacal light and background. Starting from the science requirements, the SST has then derived the mission requirements [11].

Table 1 ARIEL main science and mission requirements

Parameter	Value
Wavelength coverage	Spectral 1.95–7.80 μm Photometric 0.55–1.95 micron
Resolving power	≥ 100 1.95–3.95 μm ≥30 3.95–7.80 μm
SNR	Spectral 7/(10–20 for deep survey) Photometric 200
Photometric stability	~ 10^{-4} over an individual transit/occultation
Sky visibility	≥ 30% of the full sky at one time 10 h the same field The whole sky in 1 year
Effective collecting area	≥ 0.6 m^2
System throughput	Spectral: ≥ 40% Photometric: ≥ 50%
Detector QE	Detectors QE ≥ 50%

In Table 1, the most important science and mission requirements for the spectral and photometric observations are reported. The telescope requirements will be discussed in Sect. 4.1.

2.2 ARIEL performance requirements

A numerical end-to-end simulator of transit spectroscopy, called ExoSim, has been used to predict the ARIEL performance. It permits to simulate observations in the different observing modes, i.e., both primary transit and planetary eclipse (occultation) as well as phase curves. ExoSim inputs are: the target astronomical source parameters, the instrument parameters, and the noise sources (see Fig. 1a). The outputs are simulated FITS image files akin to a real observation [12].

The ARIEL performance is then determined by analysing these simulated data and extracting the signal and noise information, or reconstructing the planet spectrum, as it is normally done with real data [13, 14]. Since ExoSim performs a time domain simulation, it is particularly suited for capturing the effects of correlated noise (e.g., from pointing jitter or stellar variability) and time-dependent systematics. It can examine the out-of-transit noise as well as simulate full transits and obtain the uncertainty on the planet spectrum.

The impact of the stellar variability on the ARIEL data has been specifically studied with ExoSim [15], and it has been demonstrated that the ARIEL design is capable of

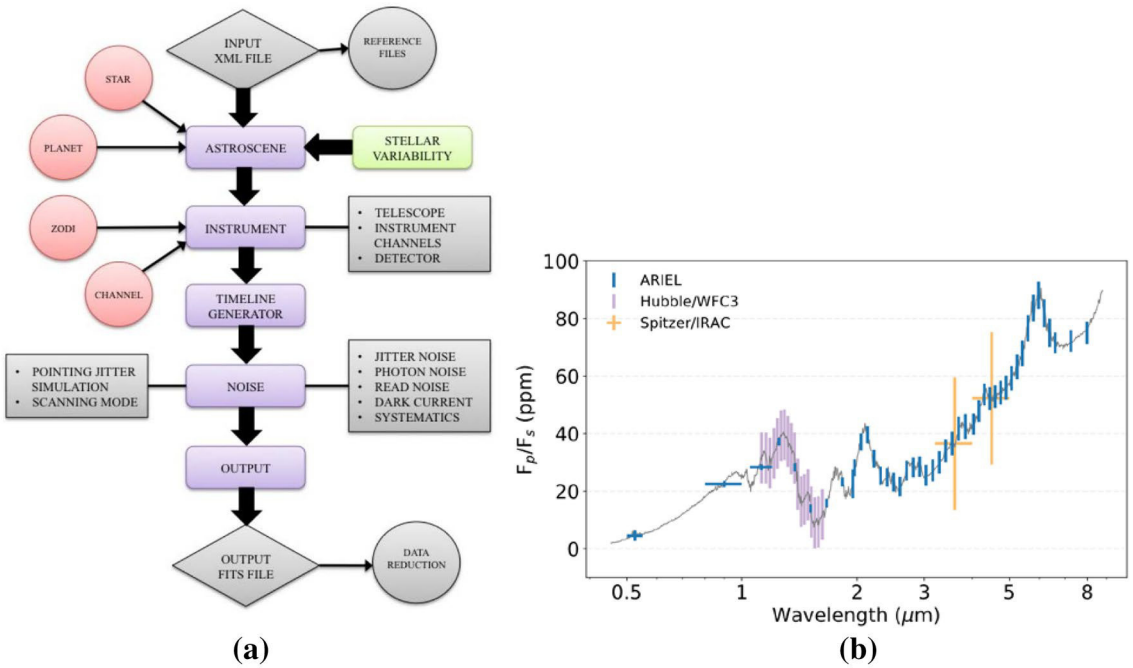

Fig. 1 In **a**, ExoSim model architecture. In **b**, expected output from the ARIEL processed data [6]

Journal : Large 12567 | Article No : 175 | Pages : 20 | MS Code : CEAS-D-17-00051 | Dispatch : 26-10-2017

achieving a very high level of photometric stability to record the exoplanet atmospheric signal, i.e., 10–50 ppm relative to the target star (post-processing). Moreover, the broad instantaneous wavelength range covered by ARIEL will allow to detect many molecular species, probe the thermal structure, identify/characterize clouds, and monitor/correct the stellar activity. To reach these goals, also requires a specifically designed stable payload and satellite platform.

An example of the expected output from the ARIEL processed data is shown in Fig. 1b. The simulated target is a hot super-Earth exoplanet orbiting around a G-type star. Data from eight simulated eclipses, i.e., about 32 h of observation, have been used. The results, with error bars, are compared to those obtainable with two current available facilities, i.e., Spitzer and Hubble WFC3.

The detailed ExoSim performance studies also show that an effective telescope collecting area of 0.6 m^2, coupled to the required system throughput and detector QE, is sufficient to achieve the necessary observations on all the ARIEL targets within the mission lifetime.

ARIEL will carry a telescope unit feeding a collimated beam into two separate modules. A combined Fine Guidance System (FGS)/Vis Photometer/NIR Spectrometer that contains three photometric channels in the wavelength range between 0.50 and 1.20 μm to monitor the photometric stability of the target stars. Two of these channels will also be used as a prime/redundant system for providing guidance and closed-loop control to the high stability pointing Attitude and Orbit Control System (AOCS) of the spacecraft (S/C). Integrated in this same module is a further low-resolution ($R = \sim 10$) spectrometer channel in the 1.20–1.95 μm waveband. This first combined module is often simply referred to as the FGS. The second module, acting as the main instrument, is the ARIEL IR Spectrometer (AIRS), providing variable resolving power in the range 30–180 for a waveband between 1.95 and 7.8 μm.

The payload is passively cooled to ~ 50 K by isolation from the S/C bus via a series of V-groove radiators. The AIRS detectors are the only items that require active cooling to < 42 K via an Ne JT cooler. While the other detectors, i.e., those for the FGS channels, will be actively stabilized at a temperature < 70 K by switching on/off their thermal control system (basically a heater).

3 Spacecraft and science payload

3.1 Spacecraft architecture

A "horizontal" configuration, with respect to the Service Module (SVM) cylinder, has been adopted as baseline for the S/C architecture (see Fig. 2). The *X*-axis of the ARIEL mechanical reference system corresponds with the telescope

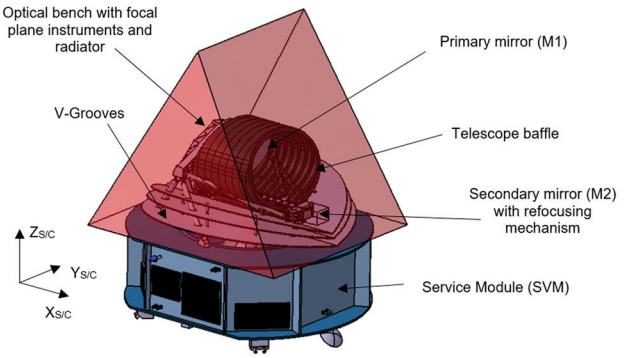

Fig. 2 Schematics of ARIEL S/C baseline configuration: main components and S/C reference system are highlighted; the red cover shows the minimum allowable volume with respect to the Sun vector

mirrors optical axis, the *Z*-axis is the launch vehicle symmetry axis ("vertical"), and *Y*-axis completes the right-handed set.

The S/C can be considered as composed of a cold Payload Module (PLM), containing the telescope and the instruments with their thermo-mechanical hardware, and a warm Service Module (SVM) that includes all the mission-supporting systems together with the PLM and cryogenic control units [16]. The PLM will interface to the SVM via a set of thermally isolating support struts, or bipods, and will be radiatively shielded from the SVM and the solar input loads by a set of 3 V-Grooves (VGs).

The sun is located below the platform (i.e., $-Z_{S/C}$). The V-grooves (see par. 3.1.3) and volumes are designed to accommodate a ± 6° angle and a ± 30° angle clearance, respectively, around the *X*-axis and the *Y*-axis with respect to the Sun vector. This solution has been taken to limit the size and mass of the VGs, which are needed to maintain the payload stable at cryogenic temperatures, and at the same time satisfying the requirements on the sky visibility. Assuming a representative operational orbit of ARIEL around L2, the complete sky is accessible within a year with any point on the sky observable for at least 4 months, and for the celestial poles, the coverage is continuous.

In Fig. 3, the sky visibility is shown. It has been indicated in fraction of a year for which a given location in the sky, expressed in equatorial coordinates, is visible. The superimposed green and red circles are the currently known best targets in terms of stellar brightness and planetary parameters (green circles are the very best), and yellow dots are known transiting planets observable by ARIEL. These current 200 known targets have been discovered mainly close to the ecliptic plane, because they are provided by ground-based surveys. K2, CHEOPS, and NGTS are expected to complete the search for planets around bright sources closer to the ecliptic plane. TESS and PLATO will extend the planet search closer to the ecliptic poles.

Journal : Large 12567 | Article No : 175 | Pages : 20 | MS Code : CEAS-D-17-00051 | Dispatch : 26-10-2017

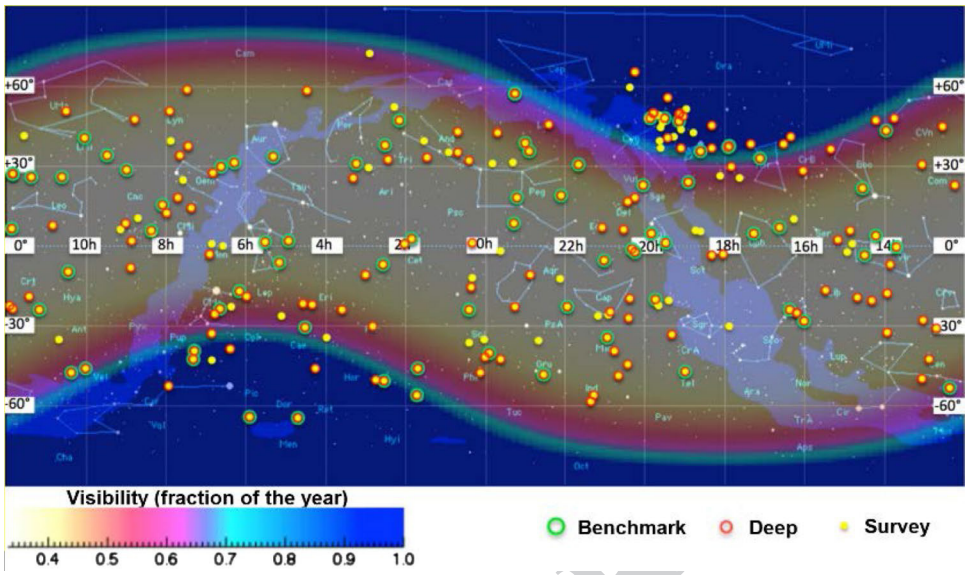

Fig. 3 ARIEL sky visibility. Fraction of the year for which a given location in the sky (in equatorial coordinates) is visible to ARIEL. Superimposed are known targets: in green, the very best, in red, the best, and in yellow, currently known transiting planets observable by ARIEL [6]

3.1.1 Cold payload module architecture

To achieve its primary objectives, the mission carries a single dedicated payload that will be developed and delivered by the ARIEL Payload Consortium [17]. A block diagram of the overall payload architecture with its subsystems is shown in Fig. 4. The ARIEL cold PLM consists of an integrated suite of telescope, spectrometers, and FGS/photometers along with the necessary supporting hardware and services (such as optical bench, cryogenic harnessing, thermal isolation structures, and active thermal stabilization control, i.e., heaters and thermistors, etc.).

The ARIEL telescope consists of three mirrors (M1, M2, and M3) having optical power plus a plane mirror (M4) used to redirect the collimated beam towards the optical bench (OB) located on the back of M1 (see Figs. 5a, 7). The secondary mirror is located at the end of a metering structure (beam) departing from the OB and it will be equipped, as a baseline, with a refocusing and tip/tilt mechanism. There will also be an eccentric baffle around M1, internal vanes between M1 and M2, M2 and M3, field and Lyot stops to

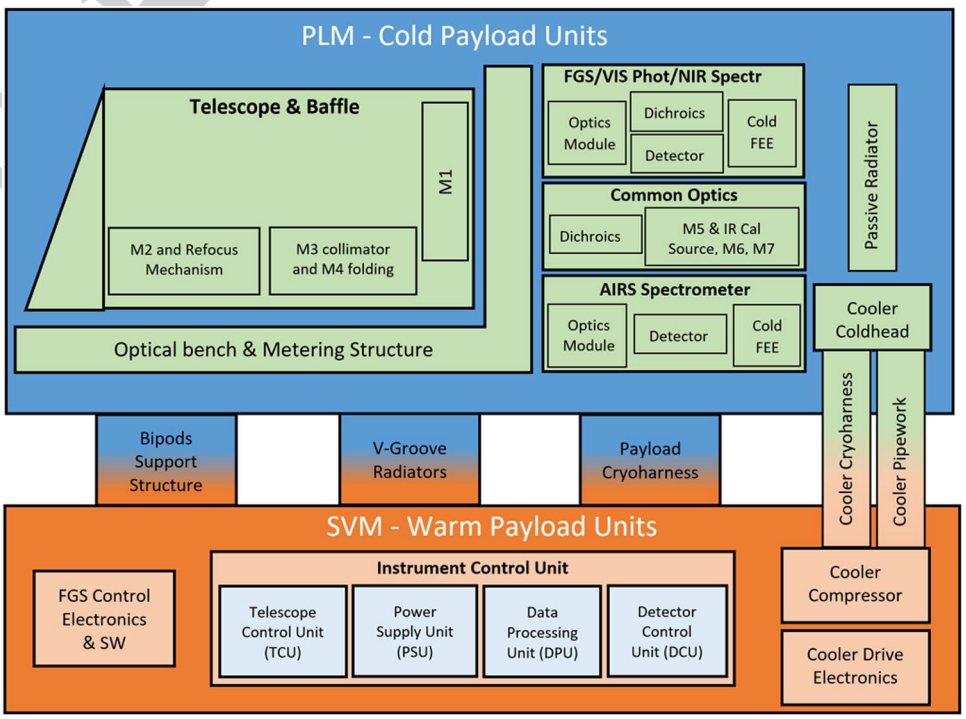

Fig. 4 ARIEL baseline payload block diagram architecture

Journal : Large 12567 | Article No : 175 | Pages : 20 | MS Code : CEAS-D-17-00051 | Dispatch : 26-10-2017

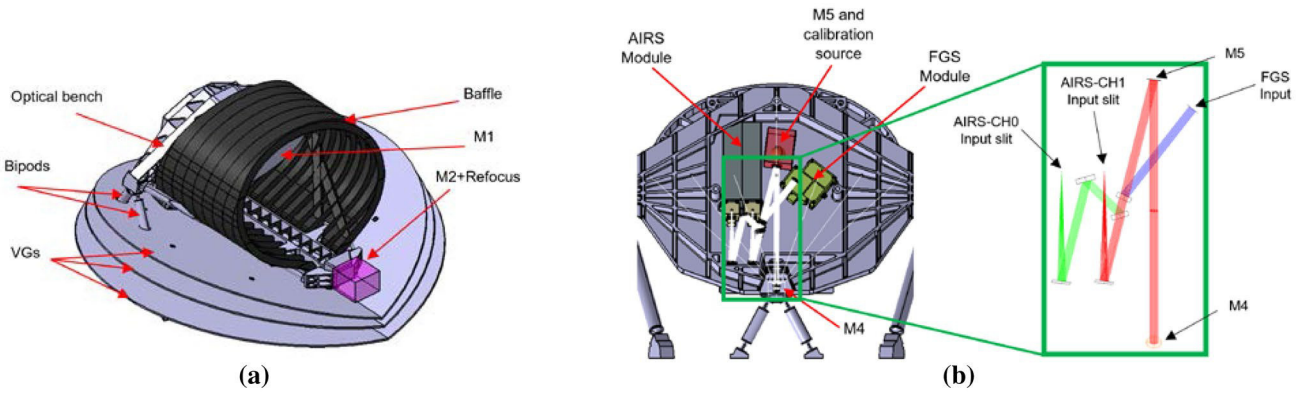

Fig. 5 In **a**, ARIEL telescope mechanical layout. In **b**, mechanical design of the OB with highlighted the optical path to the FGS and AIRS modules; in the inset, there is a zoom on the common optics region

control and limit both the out-of-field and in-field scattered stray light.

There is an additional M5 plane mirror (see Fig. 5b), which deflects the beam on the OB. Following M5, a number of plane dichroic mirrors are adopted to split the light and redirect it toward the fine guidance and spectrometer modules. These relay optics plus M5 constitute the common optics unit (COM).

Since calibration requirements are under assessment, additional hardware might be added within the instrument cavity. An IR calibration source based on the heritage of the JWST MIRI calibration system [18] and injected in the centre of the M5 mirror has been considered as the baseline solution.

The instrument modules AIRS and FGS are accommodated on the optical bench behind M1 (see Fig. 5b), enabling a direct view to deep space to provide direct radiative cooling. The units are thermally isolated by the VG shields and the critical elements such as AIRS detectors (see par. 3.2.2) are cooled by a dedicated radiator and thanks to an active cooler cold end integrated on the OB.

The detectors of the FGS, located in a single module box (the FGS box) are passively cooled to $T \leq 70$ K by a dedicated radiator represented by the top surface that closes the modules cavity on the OB. This radiator, fully enclosed in the cold radiative environment set by the last V-groove, always faces the cold space during operations. The AIRS detectors must be operated colder, below 42 K, with the goal of reaching a temperature around 36 K, to minimize detector thermal noise. Maintaining this temperature, with a load of tens of mW, requires the implementation of an active cooling system. The cryocooler baseline relies on the Planck mission and EChO study heritage: a JT cold end fed by a Planck-like mechanical compressor using Neon gas isenthalpic expansion to achieve the required low temperature and heat lift [19].

The main cold units are summarized in Table 2.

The baseline design of the PLM includes one potential active mechanisms in the payload. This is the refocusing mechanism on the telescope M2 mirror, which is used to ensure that the alignment and image quality of the telescope system are within the allowed ranges after launch and cooldown.

3.1.2 Service module architecture

The ARIEL warm units are integrated in the SVM. These include the payload electronics, which consists of three boxes that act as remote terminal units (RTUs) via Spacewire (ICU and FGS plus the cooler control electronics) to the S/C Command and Data Management System (CDMS). All commands coming from Ground, operational sequencing and data storage are managed and implemented within the S/C CDMS.

The payload warm units are summarized in Table 3.

3.1.3 PLM and SVM interfaces: V-grooves, bipods, and supporting struts

The VGs are high-efficiency passive radiant coolers and provide the first stage of the PLM cooling system. The Planck mission has definitely demonstrated their efficiency as passive cooling systems. Parasitic heat from warmer sections of the S/C is intercepted by the VGs and radiated to space after multiple reflections between the adjacent shields. To achieve this, VGs surfaces must have a very low emittance coating, i.e., a high reflection/mirroring material needed to reflect heat radiation. Only the upper surface of the last VG (VG3), exposed to the sky, is black coated with a high emissivity material to maximize the radiative coupling, and so the heat rejection to deep space. The ARIEL VG system consists of a set of three specular shields, composed of six

Journal : Large 12567 | Article No : 175 | Pages : 20 | MS Code : CEAS-D-17-00051 | Dispatch : 26-10-2017

Table 2 ARIEL cold payload units

Unit name	Unit description
Telescope assembly	Incorporating M1–M4 mirror, a refocusing and tip/tilt mechanism on the M2 mirror, the telescope optical bench, structure and baffles. Passively cooled. The M1 temperature is actively stabilized
Common optics (COM)	Including the M5 mirror, the dichroics to split the FGS and spectrometer light, the formatting optics to inject properly the light into the spectrometer, and potentially a common calibration source for the payload. COM subsystems are directly mounted on the optical bench. They are thermally controlled via the optical bench
ARIEL IR spectrometer (AIRS)	Primary science payload. Optical module with optical interface to common optics and mechanically mounted on the optical bench. Thermally controlled via the optical bench for the structure and optics and via active control system (JT cooler and the thermal control system) and cold strap to the payload radiator for the detectors Including all optics and structure plus detectors and cold front-end electronics (CFEE)
Fine guidance sensor (FGS)	Optical module with optical interface to common optics and mounted on the optical bench. Thermally controlled via the optical bench for the structure and optics and via active control system (only thermal stabilization by the thermal control system) and cold strap to the payload radiator for the detectors
ARIEL thermal hardware (ATH)	Dedicated radiator for detectors and optical module cooling plus thermal straps to provide detector interfaces. Mounted off optical bench
ARIEL cryocooler	The cryogenic active system is based on a mechanical compressor (heritage of the Planck mission) feeding a JT cold end. Neon is used as the cryogenic fluid to reach temperatures in the 28–36 K range to cool-down AIRS detectors only

Table 3 ARIEL warm payload unit

Unit name	Unit description
Instrument control unit (ICU)	Drives for spectrometer detectors and Instrument Control. Command and data handling, compression (if needed) and on-board pre-processing, formatting. I/O to CDMS. It acts as a Master for the TCU subsystem
FGS electronics (FGE)	Drives for FGS detectors and FGS module control. Command handling. Data handling, compression (if needed), on-board pre-processing and data formatting. FGS data processing. I/O to CDMS via Spacewire
Telescope control unit (TCU)	TCU is an ICU slave subsystem. Drives for heaters, thermistors (including those mounted on the OB) etc. Commands from ICU handling. Data formatting. I/O to ICU via I^2C or Spacewire TCU will be also in charge of controlling the refocusing mechanism on the M2 mirror and the IR Calibration source, thanks to its own driver sections
Cryoharness	Harness connecting warm and cold payload units including internal harnessing and mating connectors
Cryocooler compressor	The active cooling system compressor is based on a Planck-like mechanical system, with vibrations control and mitigation capabilities. Its task is to pressurize the low-pressure gas returning from the cold end feeding it back to the JT expander

half circles arranged in a "V-shaped" configuration, angled along the diameter parallel to the S/C *X*-axis (see Fig. 4). A constant angle of 7° has been assumed as the inclination between VGs, resulting in a set of 7°–14°–21° for the three shields, separated by a gap of 100 mm at the vertices. VGs are mechanically designed as a simple sandwich of aluminium alloy (series 1000 or 6000) layers. A honeycomb cell structure 10-mm thick, with 10 mm (or less) cell size and ribbon thickness of 1 mm, is packed between two 1-mm-thick layers.

The PLM is supported by three bipods mounted onto the PLM/SVM interface plate. One bipod is centrally positioned at the front of the telescope baffle. The other two are on the rear side of the Telescope Assembly, supporting the OB and the baffle on two points. The VGs are also mechanically and thermally attached to the three bipods plus the extra support provided by eight auxiliary struts (TBC). The need for these extra supports and their thermo-mechanical design will be investigated in the next phase of the analysis. Bipods preliminary thermo-mechanical configuration is based on the Planck design. They are assumed as hollow cylinders made of GFRP (R-Glass + Epoxy), a low conductive material with good structural properties. To increase their mechanical stiffness, the inner volume of the cylinders is filled with low thermally conductive rigid foam. The eight extra supporting struts for the VGs are positioned in the outer boundary part of the PLM to support the radiators' edges. They are designed as hollow GFRP cylinders extending from the SVM/PLM interface to the lower surface of the last VG.

Journal : Large 12567 | Article No : 175 | Pages : 20 | MS Code : CEAS-D-17-00051 | Dispatch : 26-10-2017

3.2 Science payload

As already mentioned, the science payload, in its cold part, is composed of: a telescope unit, a spectrometer unit and a fine guidance unit. The telescope will be described in the next paragraph. The primary payload is the spectrometer, whose scientific observations are supported by the fine guidance system and photometer, which is monitoring the photometric stability of the target and allowing, at the same time, the target to be properly pointed.

In particular, to achieve the required photometric stability, a good pointing stability needs to be provided by the S/C during an observation. For this purpose, the FGS channels looking to the target star in parallel to the spectrometer will be accommodated on the payload and used by the AOCS.

Both the spectrometers and FGS will be mounted on the common OB.

3.2.1 FGS and its objectives

The Fine Guidance System (FGS) main task is to ensure the correct pointing of the satellite, to guarantee the target star is well centred on the spectrometer slit during all the observation sessions. It will also provide high precision astrometry, photometry, and spectro-photometry of the target for complementary science. In particular, the data from the FGS will be used for de-trending and data analysis on ground. The sensor uses star light coming through the optical path of the telescope to determine the changes in the line of sight of the ARIEL instrument. The attitude measurement is then merged with the information from the star tracker, and used as input for the control loop stabilizing the S/C through the high performance gyros.

To meet the goals for guiding and photometry, four spectral bands are defined:

- FGS 1: 0.8–1.0 μm,
- FGS 2: 1.05–1.2 μm,
- Vis Phot: 0.50–0.55 μm,
- NIR-Spec: 1.25–1.90 μm including a prism element with low spectral resolution greater than 10.

The instrument has two detectors: one is shared by the FGS1 and Vis-Phot channels and the other one by the FGS2 and NIR-Spec channels. The baseline detectors are the standard substrate removed Teledyne H1RG [20], 2.5 μm cut-off wavelength, and 1024 × 1024 pixels with 18 μm pixel pitch. They have a QE greater than 50%, high technology readiness level (TRL) (9) and space heritage.

The information from all the FGS channels is used as a stellar monitor and to provide photometric information to constrain the Vis/NIR portion of the exoplanet spectra. The information from one of the FGS channels will be used as the nominal FGS information to feed into the AOCS. In case of failure in the system, then the information from the other channels can be used. The spectral bands are selected from the incoming light using dichroic filters.

The main requirement of the FGS is the centroiding performance of 10 milli-arcsec at 10 Hz to achieve centroiding to 1/10th of a pixel level. For the best support of the operating modes, several centroiding and data extraction algorithms will be implemented, fully configurable by parameter and command.

The FoV of the FGS on sky is: 17″ × 17″ as the internal field, usable for centroiding and 25″ × 25″ as the outer full field maximum usable on sky, which corresponds to an internal FGS FoV of ± 0.19°. For the different channels, the plate scale ranges between 6 and 9″ per pixel (for further details, see [21]).

The FGS could also be used during the commissioning of the payload to iterate and optimize the telescope focus and spherical aberrations by an iterative loop (with ground control) feeding into the M2 mirror mechanism. To support this activity, a dedicated PSF imaging mode can be envisaged.

3.2.2 ARIEL IR spectrometer (AIRS)

The prime science payload for ARIEL is a broadband, low-resolution NIR and MIR spectrometer operating between 1.95 and 7.80 μm. The IR spectrometer can be split into multiple channels but not at wavelengths with key spectral features for which overlapping on different channels is needed for spectra retrieval.

The baseline design foresees two spectrometers with independent optical channels and detectors: the first one (CH0) covering the shorter waveband (1.95–3.90 μm), the second (CH1) the longer waveband (3.9–7.8 μm). As dispersive element, prisms have been considered in the present design.

The beam reaching the AIRS slits has an F#18 in the spectral direction and F#12 in the spatial direction. The pixel scale of each AIRS channel depends on their optical design, i.e., on the focal lengths of the collimator and of the camera. The focal length of the cameras is different for the two channels. Some of the AIRS characteristics are reported in Table 4. For full details and complete AIRS performance predictions, see [21].

The baseline detectors for AIRS, as well as for the FGS, are the hybrid CMOS substrate removed H1RG from Teledyne. Given the different wavelength range, they have different cut-off wavelengths. The CH0 detector is an H1RG standard type with a 5.3 μm cutoff, while the CH1 detector is a custom NEOCam type [22], operated at a temperature of ~ 36 K using an active cooling system.

Journal : Large 12567 | Article No : 175 | Pages : 20 | MS Code : CEAS-D-17-00051 | Dispatch : 26-10-2017

Table 4 Summary of the main AIRS characteristics

	Waveband (microns)	Slit size spatial direction	Spatial scale (″/px)	Slit size spectral direction	Spectrum size (px^2)	Resolving power
CH0	1.95–3.90	1.26 mm (20″)	0.22	0.296 mm (4.7″)	270 × 64	100–180
CH1	3.90–7.80	1.26 mm (20″)	0.45	0.465 mm (7.4″)	100 × 64	30–65

Table 5 Summary of the telescope optical requirements

Parameter	Value
Collecting area	> 0.6 m^2
FoV	30″ with diffraction limited performance 41″ with optical quality TBD allowing FGS centroiding 50″ unvignetted
WFE	Diffraction limited @ 3 μm
Wavelength range	0.55–8 μm
Throughput (EOL)	Minimum > 0.78 Average > 0.82
Output beam dimension	20 mm × 13.3 mm

For the AIRS, only a part of the detector will be used for detecting the spectrum as the spectrum size (see Table 4) is significantly smaller than the detector area.

Another option, presently considered for the detectors both for FGS and AIRS, is the adoption of European MCT detectors. In fact, there are specific efforts underway within Europe (CEA/LETI) to develop a detector (640 × 512 or 320 × 256, 15 μm pixels) with cut-off wavelength at 8.2 μm at 45 K.

4 Telescope optical design

4.1 Telescope design requirements

The telescope optical layout has been designed to provide the optical requirements, as reported in Table 5, which have been derived by the mission requirements [11]. The requirement on the collecting area of 0.6 m^2 implies an entrance pupil of the order of 1 m in diameter. The collecting area is related to the minimum intensity (magnitude) of the observable targets.

The design performance is driven by the requirement that the final as-built quality of the telescope system has to be diffraction limited at 3 μm over an FoV of 30″, i.e., equivalent to an RMS wavefront error (WFE) of 220 nm.

The requirement on the telescope throughput has been derived by breaking down the global system throughput budget and including the lifetime degradation. The broken-down budget ensures that all the channels are compliant with the mission requirements [21] [23]. To guarantee the required throughput without increasing the size of the primary mirror, that is the entrance pupil of the telescope, the optical design has to be unobscured. The unobstructed solution also assures that the energy in the PSF is primarily contained inside the first Airy disk and not spread towards the secondary rings [24].

The wavelength coverage and the global FoV of the telescope are determined by the requirements on the instruments following the telescope, i.e., the FGS and the AIRS.

4.2 Telescope FoV determination

In the determination of the FoV for the telescope, there are three aspects to consider: the FoV required for the FGS, the FoV required for the AIRS, and the FoV required for the telescope itself. For each of these not, only the nominal scientific FoV has to be taken into account, but also the extended FoV needed for accounting for misalignment [absolute performance error (APE)] or for channel calibration. For example, in the spatial direction of the AIRS, an extended FoV is needed for monitoring the background (i.e., zodiacal and thermal background but also detector dark current). The FGS has to be able to acquire the source also in the "coarse alignment mode", i.e., before the fine guidance loop has been closed, which implies a larger FoV for the telescope.

Moreover, an additional FoV requirement of 10″ is intended to allow for off movements of the telescope with respect to the instrument optical bench (for example, due to launch loads, settling of the structure post-launch and dimensional changes on cooldown).

A 26.4″ diffraction limited telescope FoV is required to ensure that there is a well-resolved PSF at the centre of the spectrometer slit. A larger 37″ telescope FoV is required to allow the FGS to acquire a star and centre it on the slit. The image quality level over this 37″ annulus is still to be defined, but it can be of lower quality, sufficient to allow the star centroid to be well enough resolved to be initially located and then brought to the centre of the FGS FoV, where the telescope image quality is better. This annulus has been indicated as the 'FGS acquisition' FoV. A still larger

Journal : Large 12567 | Article No : 175 | Pages : 20 | MS Code : CEAS-D-17-00051 | Dispatch : 26-10-2017

telescope FoV, extending to 46″, is required to capture the slit background. There are no image quality requirements over this additional FoV; the only real requirement is for the FoV to be unvignetted, so that background photons reach the slit. This annulus has been referred to as the 'background' FoV.

However, this situation does not allow any margin for misalignment of the FGS and AIRS. They must be co-aligned to better than ± 5″ in any case, or else the PSF cannot be located on the centre of the slit and in the FGS FoV at the same time. Some margin is also needed to allow to account for the fact that the telescope to OB alignment will be set to some datum on the optical bench, and there may be some residual misalignment between that datum and the individual FGS and AIRS instruments. It is reasonable to suppose that these misalignments will be small in comparison with the offset between telescope and OB, given that AIRS and FGS will be integrated on a single optical bench.

For the moment, it has been assumed that both the FGS and AIRS will be aligned to a datum on the instrument optical bench (for example, an optical reference cube) to within ± 2″, implying a maximum co-alignment error between the two of 4″. This reference cube has been assumed as the datum to which the telescope is aligned. This implies that a 4″ margin on all of the telescope FoVs must be added to allow for these alignment errors. This gives the final telescope FoVs, as shown in Fig. 6 and summarized in Table 6.

4.3 Telescope design characteristics

The baseline telescope design is an afocal unobscured eccentric pupil Cassegrain telescope (M1 and M2) with a recollimating off-axis parabolic tertiary mirror (M3). All the mirrors share the same optical axis. An M4 plane mirror is redirecting the exiting beam parallel to the back of M1, where the OB is located and the instrument will be mounted (see Fig. 7).

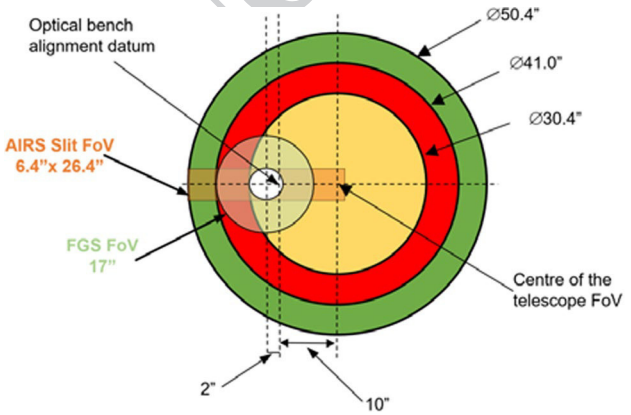

Fig. 6 Final telescope FoV. All dimensions are to scale

Table 6 Summary of FoV requirements

Designation	FoV (arcsec)
AIRS	6.4 × 26.4
FGS	17
Telescope: Diffraction limited	30
Telescope: FGS acquisition	41
Telescope: Background	50

Telescope FoV values are rounded to the nearest arcsec

Note that the optical reference system (shown in Fig. 7) is different from the S/C one. The telescope is accommodated horizontally with its optical axis (*Z*) along the S/C *X*-axis. The centre of the FoV of the telescope is inclined of 0.1° in the *YZ* plane with respect to the optical axis of the telescope defined by the mirrors common optical axis.

The system aperture stop/entrance aperture is located at the M1 surface. The M1 aperture is an ellipse with major/minor axes dimensions of 1100 mm × 730 mm. The complete characteristics of the optical design are summarized in Table 7a, while in Table 7b, the parameters (radius of curvature, conic constant, off-axis, etc.) of the telescope mirrors are described.

The value of the angular magnification is forced by the need to conjugate the M1 aperture size with the desired output beam dimension at the exit pupil.

To be able to satisfy the required telescope throughput, a protected silver coating has been adopted as baseline for the mirror surfaces. In fact, silver coatings are able to provide more than 96% of reflectivity both in the UV and IR wavelength regions. Many researches have been done, or are in progress, for studying and improving the high reflective coatings for space applications, and in particular the protected silver ones [25–27].

A detailed trade-off for the material to be used for the telescope mirrors, specifically for M1, and telescope structure has been carried out during the ARIEL assessment phase. The conclusion is that for the consortium provision of the telescope, the optimum solution is a telescope with mirrors and structure made from aluminium 6061 T651 alloy [28]. The viability of using aluminium as the baseline material for the telescope mirrors has been assessed during phase A by producing a pathfinder M1 mirror [21].

The primary mirror will be lightened and its mechanical shape is studied to give high bending stiffness both during manufacturing and in operating condition. The selected mounting system ensures isostatic thermal fixation of the primary mirror. M1 is supported directly by the OB via a nine-point whiffletree structure, which is connected to the OB via three triangular mountings. The M1 mechanical configuration is shown in Fig. 8.

Journal : Large 12567 | Article No : 175 | Pages : 20 | MS Code : CEAS-D-17-00051 | Dispatch : 26-10-2017

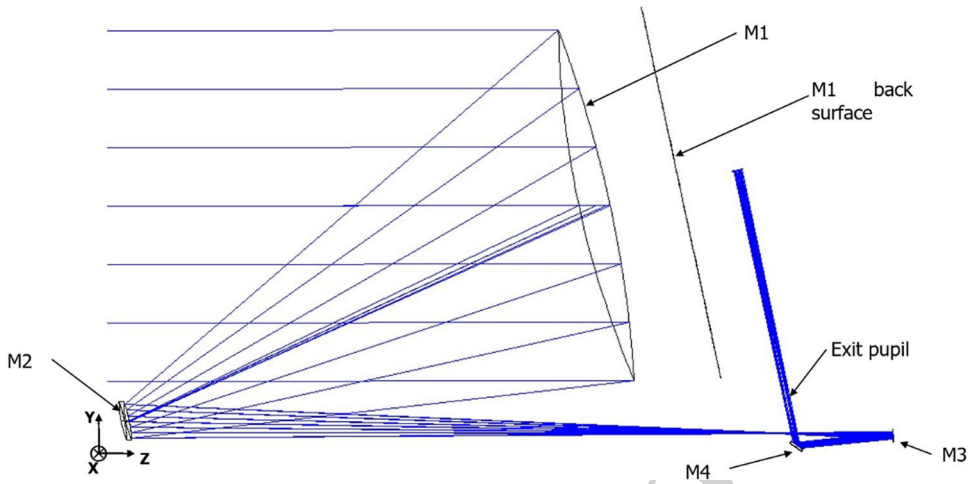

Fig. 7 Scale drawing of the telescope—view in *Y*–*Z* plane

Table 7 (a) Summary of the telescope optical design characteristics, (b) mirror parameters description

(a)

Parameter	Values
Optical concept	Eccentric pupil Cassegrain telescope plus off-axis paraboloidal mirror and folding. Afocal design
Focal length	14.17 m
FoV centre	0.1—off-axis *YZ* plane
Pupil size	Ellipse with major axis 1.1 m × 0.73 m
Focal ratio @ intermediate telescope focus	13/19.4
Angular magnification	− 55

(b)

Optical element	M1	M2	M3
R (mm)	− 2319.5	− 239.0	− 491.5
k	− 1	− 1.4	− 1
Off-axis (mm) (*y* direction)	500	50	20
Clear aperture radius (mm)	Elliptical, 550 (*x*) by 365 (*y*)	Elliptical, 56 (*x*) by 40 (*y*)	Elliptical, 15 (*x*) by 11 (*y*)
Type	Concave mirror	Convex mirror	Concave mirror

A static analysis has been done to assess the deformation of the M1 surface due to gravity. Different mounting plate materials have been considered. With an Al 6061 mounting plate, the expected surface distortion PTV is of the order of 100 nm, which corresponds to approximately 40 nm RMS.

4.4 Telescope optical performance

The raytracing analysis and design optimization have been done by means of the raytracing software Zemax®. To assess the quality of the telescope and determine the optical performance, since the telescope is afocal, the spot diagrams can be given using an ideal focusing paraxial lens with a defined focal length, or using the afocal image space option appropriate for systems with collimated output. Note that the

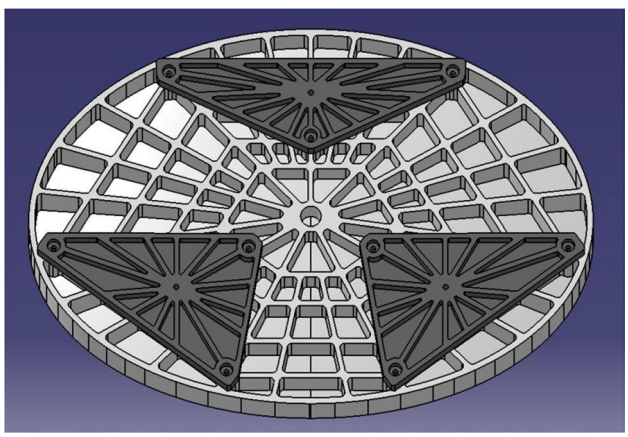

Fig. 8 Primary mirror rear side with the foreseen mounting scheme

Journal : Large 12567 | Article No : 175 | Pages : 20 | MS Code : CEAS-D-17-00051 | Dispatch : 26-10-2017

spot diagrams obtained with this second method have their size expressed in milliradians units.

The nominal diffraction PSF at 3 μm wavelength has an Airy radius, respectively, of 0.2 and 0.29 mrad in the *X*- and *Y*-directions. A picture of the expected theoretical PSF is depicted in Fig. 9a; in Fig. 9b for comparison, the spot diagram all over the 50″ unobstructed telescope FoV is drawn and compared with a box of 0.4 mrad size, so to show that telescope design is diffraction limited at the 3 μm primary wavelength.

The telescope RMS WFE is always less than 26 nm over the 30″ nominal telescope FoV (see Fig. 10); this value is well below the telescope diffraction limit at 3 μm, i.e., 220 nm.

To assess the final performance of the as-built telescope and its variation during the operation in flight, a tolerance analysis has been done [21, 29, 30]. The telescope has been considered to be designed, realized, and integrated at room temperature in 1 g environment according to the raytraced theoretical layout. Being an all-aluminium instrument, it is expected to scale down when cooling down at the nominal operating temperature. To compensate for residual mechanical deformation of the telescope due to the cooling process, the secondary M2 refocusing mechanism can be used.

The tolerance analysis has taken into account the different parts of the realization and life of the instrument:

1. manufacturing, integration, and alignment;

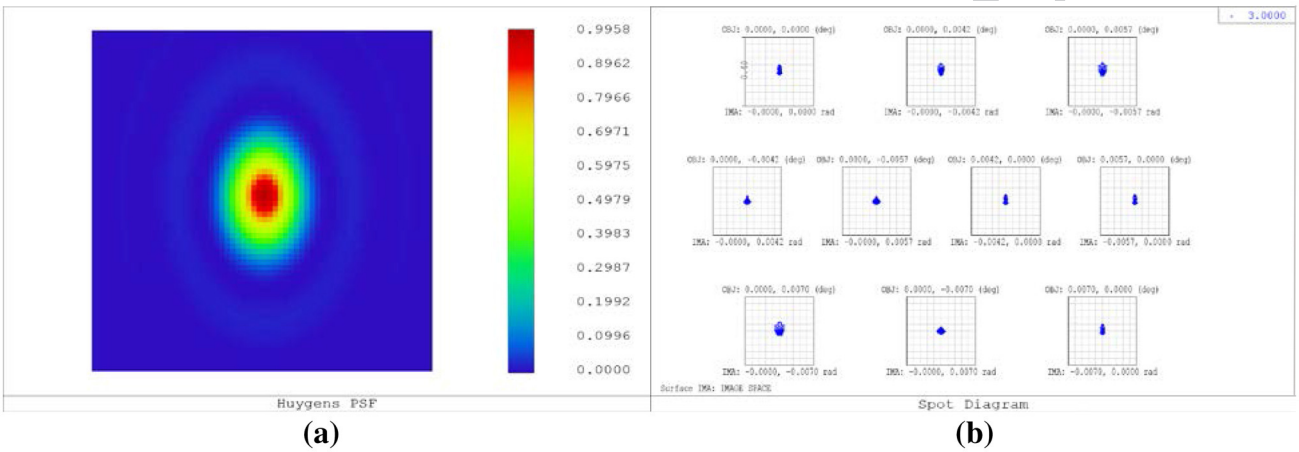

Fig. 9 In **a**, PSF calculated at the telescope FoV centre for a wavelength of 3 μm depicted over a 1 mrad square box. In **b**, spot diagrams in the afocal space; the scale (box) is 0.4 mrad

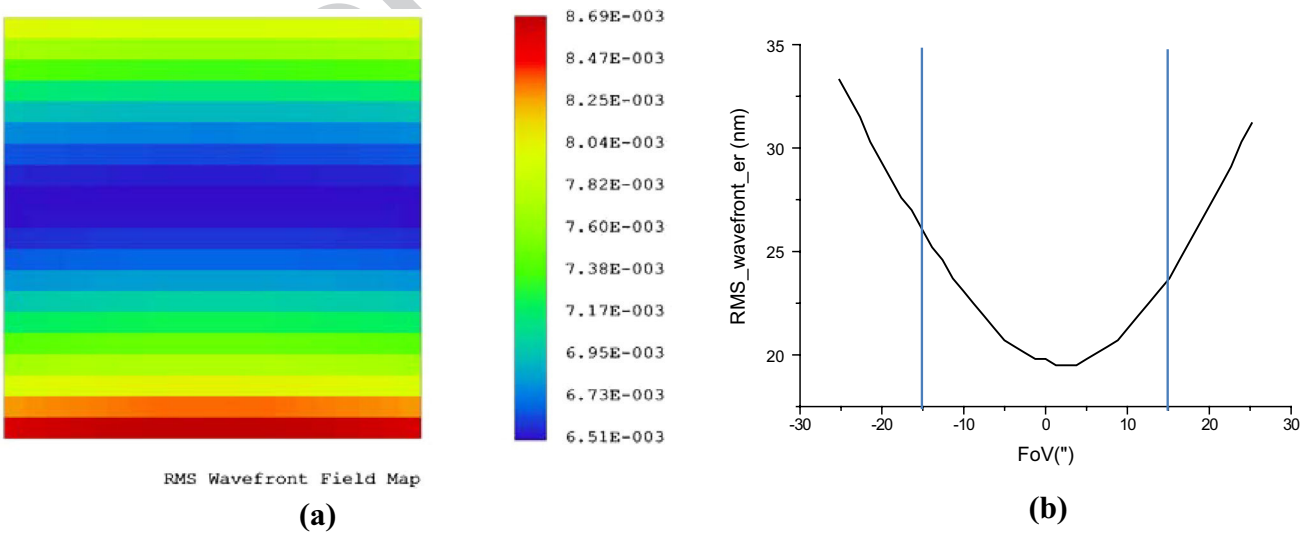

Fig. 10 In **a**, RMS wavefront error field map calculated for the 3 μm wavelength over the 30″ nominal telescope FoV. Units are λ. In **b**, cross section along the *Y* direction of the RMS wavefront error expressed in nm; in the *X*-direction, the wavefront error is constant

Journal : Large 12567 | Article No : 175 | Pages : 20 | MS Code : CEAS-D-17-00051 | Dispatch : 26-10-2017

2. launch loads and change from 1 to 0 g;
3. cooldown in orbit from ambient temperature to the nominal (about 50 K) operating temperature;
4. stability in flight: short term (over one single exposure to about 10 h) and long term (over the whole mission operative lifetime).

For the manufacturing, integration and alignment phase optical element standard manufacturing and mounting tolerances have been considered. The mirrors are foreseen to be equipped with a reference cube, or reference surfaces, and with respect to these references, the mirror local axis will be measured with high precision (~ 10/20 μm in position and 2/4″ in rotation). If after manufacturing, M1 will be measured and found to be out of the specifications; to avoid the time consuming process of re-working a 1 m diameter mirror, the possibility of re-optimize M2 will be considered. The total impact of the manufacturing, integration, and alignment process on the RMS WFE is expected to be of the order of 40 nm.

The adopted alignment philosophy is to mount M1 and, then, with the help of the reference surfaces, measure its positon and orientation and use M2 as compensator to recover the optical quality. After the telescope alignment, the boresight direction will be measured with respect to the instrument reference cube, for example, using a theodolite setup [31], and used to co-align the other ARIEL modules.

To reduce the deformation effects induced by gravity during the alignment and tests on-ground, a slightly inclined position of the telescope, with the gravity acting parallel to the optical bench, is suggested to be adopted. The whole telescope structure should be rotated about 12° with respect to the telescope interface to SVM [21].

A preliminary thermoelastic analysis has been performed to verify the deformation of the primary mirror and the telescope structure during the cooling phase from ambient 293 K to the operating temperature. The considered operating temperature map is the one calculated using the thermal model for the reference worst case condition ("Cold Case", see the following section). The obtained resulting deformations are reported in Fig. 11. The variation of the distance between the centres of primary and secondary mirrors is of about 20 μm along the *X*-direction, about 600 μm and 4.7 mm, respectively, in the Y and Z ones. These numbers are in line with the expected displacements; in fact, the mean Al6061 coefficient of thermal expansion (CTE) in the considered temperature range is about 17 μm/m/°.

Choosing some reference points (nodes) on the primary and secondary mirrors and comparing the node expected positions, calculated with the simple scaling of the design, with the ones derived by the thermoelastic analysis, the residual deformations of the telescope have been derived. The telescope results to be rotated approximately 4′ around the *X*-axis, the distance between M1 and M2 is about 200 μm more than expected, and the estimated variation for the shape of the primary mirror is about 20 μm PTV. The first effect can be recovered re-orienting the whole S/C, the second, and partly the third, by moving M2 via the refocusing mechanism. The residual WFE after refocusing is expected to be of the order of 200 nm.

For the stability in flight, at present, the foreseen seasonal changes are estimated to be less than 1 K corresponding to an expected RMS WFE of about 130 nm. Anyway, if considered necessary, the M2 refocusing mechanism can be used from time to time to recover the WFE changes. During one single exposure, i.e., up to 10 h, the temperature variation is negligible of the order of a few mK. The induced boresight errors will be recovered using the FGS.

The results of the whole tolerance analysis show that the telescope, thermally stable after cooldown and refocused via M2 mechanism, will have a WFE of the order of 220 nm RMS. The total RMS WFE error in flight, including the stability, will be within 250 nm. Comparing these results and the WFE budget, detailed in [21], it can be demonstrated that the telescope assembly will deliver the required optical quality suitable to achieve the scientific purpose of the instrument.

5 Telescope thermal analysis and control

The telescope is passively cooled to ≤ 70 K and its thermal control is based on a passive/active approach. A high-efficiency thermal shielding system (see Fig. 12) based on a multiple radiators configuration can provide stable temperature stages down to 50–60 K in the L2 orbit environment.

The telescope baffle provides a large radiator area with a good view to deep space; this provides sufficient radiative cooling to dump the parasitic loads from the PLM support struts, cryoharnesses, and radiative load from the final VG. Temperature control of the mirrors is achieved by partial thermal decoupling from PLM units: each mirror is mounted on its supporting structure by insulating struts with a total conductance of less than 0.1 W/K. This configuration will help in filtering out all potential instabilities with periods of the order of 10–100 s originated in the PLM.

For the primary mirror, the high thermal capacitance, due to its mass, will allow a higher level of passive filtering, damping instabilities at lower frequencies, i.e., with periods of the order of few hours. The slower fluctuations, with periods of the order of several hours or longer, that could be transmitted to the optics will be smoothed by the active control system based on a proportion–integral–derivative (PID)-type feedback loop.

The telescope will also incorporate contamination control heaters on the M1 and M2 mirrors and on the PLM

Journal : Large 12567 | Article No : 175 | Pages : 20 | MS Code : CEAS-D-17-00051 | Dispatch : 26-10-2017

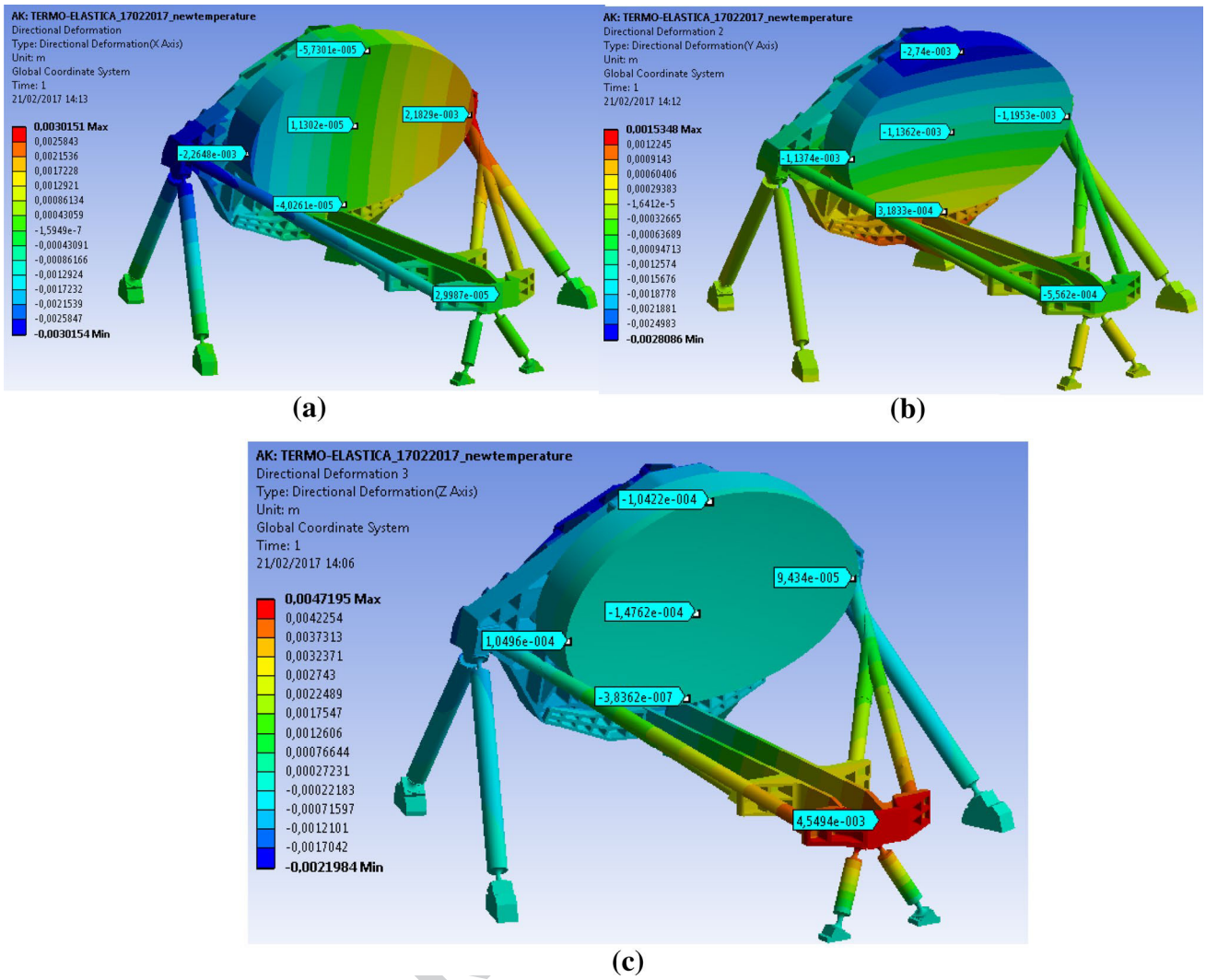

Fig. 11 In **a**, **b**, and **c**, telescope directional deformations, respectively, along the *X*-, *Y*-, and *Z*-axes resulting from the thermoelastic analysis. Units are meters

optical bench. These heaters will be active during the early orbit operations to ensure that the sensitive optical surfaces remain warmer than the support structure through the critical parts of cooldown. A temperature delta of ~ 40 K will be maintained between the baffles, which will act as a contamination getter for water and other contaminants being off-gassed by the PLM, and the optical surfaces. A preliminary calculation of the power required to maintain this temperature gradient shows that approximately 100 W of heater power is required during this phase. This would hold the sensitive surfaces at 200 K, while the baffle cools below 160 K, where the H_2O will freeze out.

A thermal analysis has been performed at PLM level. Both steady state and transient studies have been carried out for different boundary conditions on the SVM top plate and SVM radiative shield. The expected steady-state temperatures in the nominal operating conditions, corresponding to the S/C orbiting around the Sun–Earth L2 point, have been calculated as well as transients induced by an abrupt change of the boundary conditions. In addition, the cooldown from ambient temperature to the operative condition in orbit, calculated over a 30 days period, has been simulated [32].

As a reference, the steady-state results obtained for the cold PLM in the coldest operative case ('Cold Case') are shown in Fig. 13. The 'Cold Case' corresponds to the situation in which the payload reaches the lowest temperature resulting in the worst condition for what concerns the thermoelastic deformation effects on the payload. The temperatures reached by all passively and actively cooled units are fully compliant with the requirements including margins. Figure 13a shows the temperatures of the radiator, OB, and baffle, while Fig. 13b shows those of the AIRS and FGS CFEEs, detectors, and the JT cold end. Figure 14 reports a detailed view of the telescope assembly temperatures.

Journal : Large 12567 | Article No : 175 | Pages : 20 | MS Code : CEAS-D-17-00051 | Dispatch : 26-10-2017

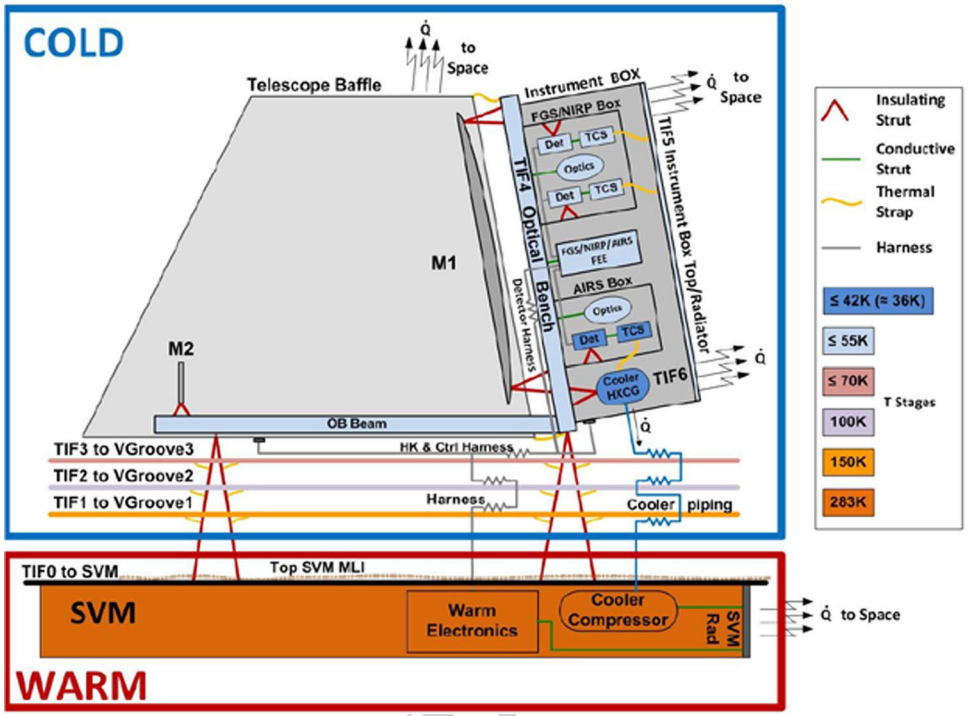

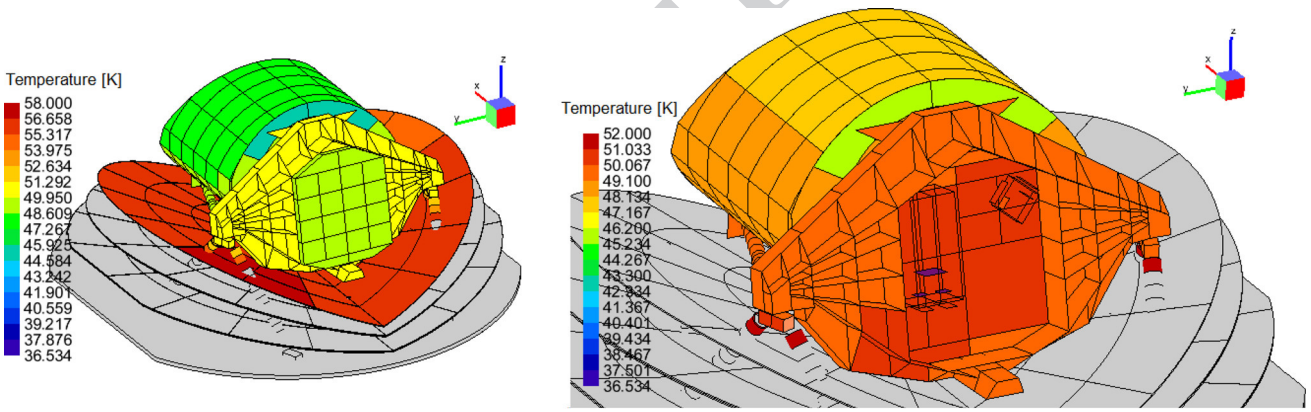

(a) (b)

Fig. 12 PLM thermal architecture scheme

Fig. 13 Thermal analysis results for the cold PLM in the steady-state 'Cold Case' in operating conditions. In **a** radiator, OB and baffle temperatures are visible. In **b**, the module boxes are hidden to show the AIRS and FGS CFEEs, detectors, and the JT cold end temperatures

Thermal stability is one of the key issues of the ARIEL PLM thermal design. For this reason, an analysis case has been computed to check the impact on the PLM of a temperature variation of 10 K of the SVM platform conductive interface during a nominal observation run of 10 h. The corresponding total change (over the 10-h period) of the M1 node temperatures is less than 0.5 mK, even in the case of a sudden change (step function) or of a linear variation imposed at the SVM interface. The preliminary results of the analysis on the cooldown show that after 30 days, the passive cooldown is concluded and the system can be considered in a steady-state thermal condition.

Summarizing the results of the thermal analysis, in routine science operation, M1 operates at a temperature around 50 K with a very high level of thermal uniformity, better than 10 mK (see Fig. 14), achieved by passive cooling. Even for the whole Telescope Assembly, the total gradient between the mirrors and the structures results limited, of the order of 2 K, considering the dimension of the system. Moreover, transient simulations show that the telescope design, with

Journal : Large 12567 | Article No : 175 | Pages : 20 | MS Code : CEAS-D-17-00051 | Dispatch : 26-10-2017

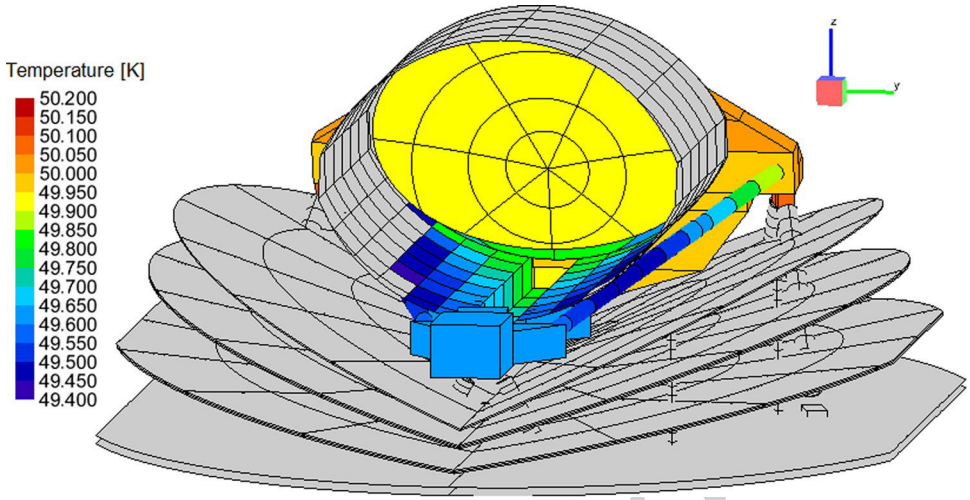

Fig. 14 Telescope assembly node temperatures in the 'cold case'

the expected levels of temperature fluctuations on the SVM interface and on the OB, is already capable of filtering out most of the thermal instabilities down to oscillations of the M1 of the order of 1 mK or less.

Anyway, the implementation on M1 of a fully redundant thermal control system (electrical resistances plus thermistors), fed by a PID-type loop control logic driven by the TCU, is at present expected to ensure thermal stability even in the presence of oscillations with a wider frequency spectrum [21].

6 Instrument control unit

The ARIEL ICU is the main electrical subsystem belonging to the payload and designed to control the spectrometer, the AIRS detectors, and the M1 active thermal system. It is also in charge of the thermal monitoring of the main PLM elements by means of its subunits, like TCU, for which ICU acts as the master logic [33]. It is linked to the S/C DMS (Data Management System) by means of two Spacewire (SpW) links.

The ICU hosts a rad-hard processor running the payload's Application SW (ASW), which mainly performs the scientific data processing, the subsystems housekeeping (HK) collection, and the Instrument Control and fault detection, isolation and recovery (FDIR) functions. Its electrical architecture includes five (active or switched on at the same time) nominal subunits:

- 1 PSU—power supply unit (nominal and redundant 3U boards);
- 1 DPU—data processing unit (nominal and redundant 6U boards);
- 2 DCU—detector control unit (only nominal 6U boards);
- 1 TCU—telescope control unit (nominal and redundant 3U and 6U boards)

as represented in Fig. 15 by grey-shaded rectangles, with blue labels for nominal (N) boards and red labels for redundant (R) boards. Actually, ICU and TCU are hosted by two stacked and independent boxes, as shown in Fig. 16 (ICU box including PSUs, DPUs, DCUs, and TCU box, as ICU slave).

ICU and TCU are provided by different countries; in particular, ICU will be designed and delivered by Italy while TCU by Spain. For this reason and to facilitate testing and AIT/AIV activities at system and subsystem level, the stacked boxes configuration has been chosen as baseline for the unit's mechanics.

The two boxes are electrically connected by means of external interface (I/F) (harnessing) exploiting front panel connectors. Both ICU and TCU boxes implement their own back panel for routing power and signal lines connecting the internal electronics boards. Alternatively, they can exploit external wired connections, but this solution would require a larger envelope, beyond the allocated volume by ESA. At the present time (several months before M4 Mission Selection Review), to also minimize the length and the mass of the harnessing connecting the two boxes, a stacked configuration is assumed.

The ICU overall electrical architecture is driven by the adoption of US detectors (H1RG type, already developed for the NASA NeoCAM IR Mission) and cold front-end electronics (CFEEs) from Teledyne (SIDECAR ASIC), given their very high TRL and space heritage with respect to the present European alternative (a Sofradir/CEA-LETI design [34]). The SIDECAR solution as CFEE is the best one to drive properly the US MCT (HgCdTe) detectors and to save mass, volume, and power at the same time. They can work easily down to the ARIEL required cryogenic temperatures

Journal : Large 12567 | Article No : 175 | Pages : 20 | MS Code : CEAS-D-17-00051 | Dispatch : 26-10-2017

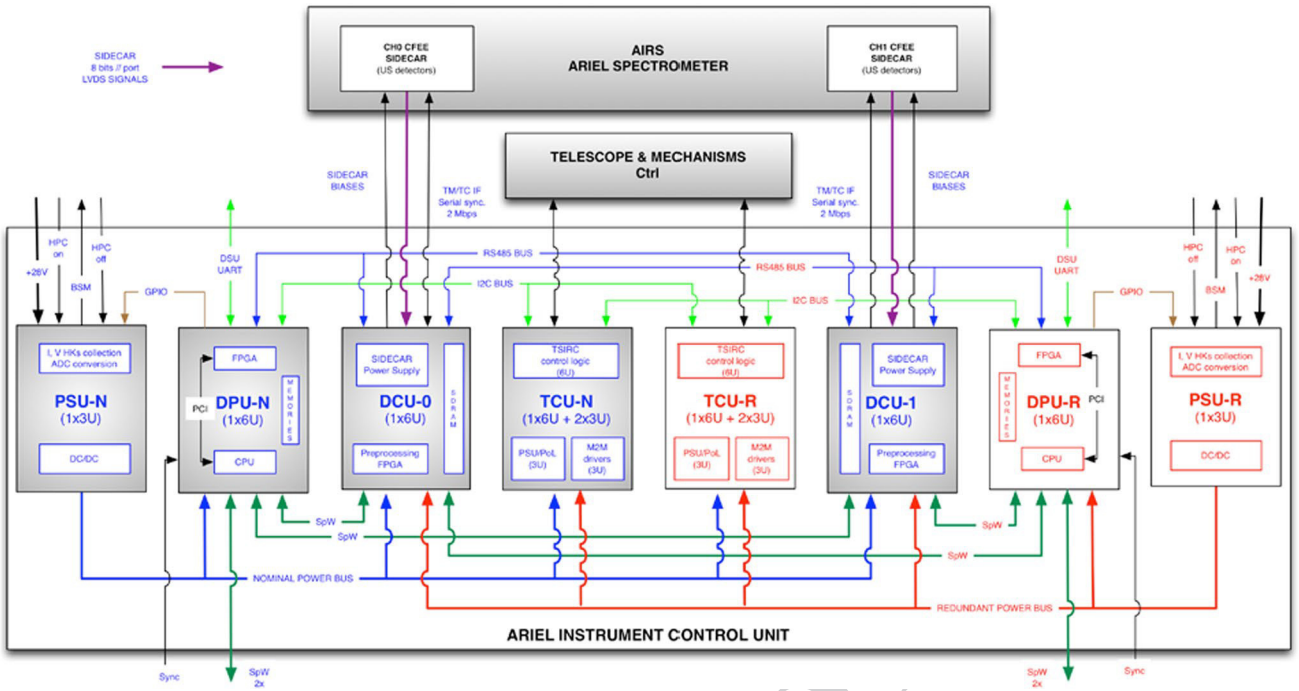

Fig. 15 ARIEL ICU block diagram and electrical I/F

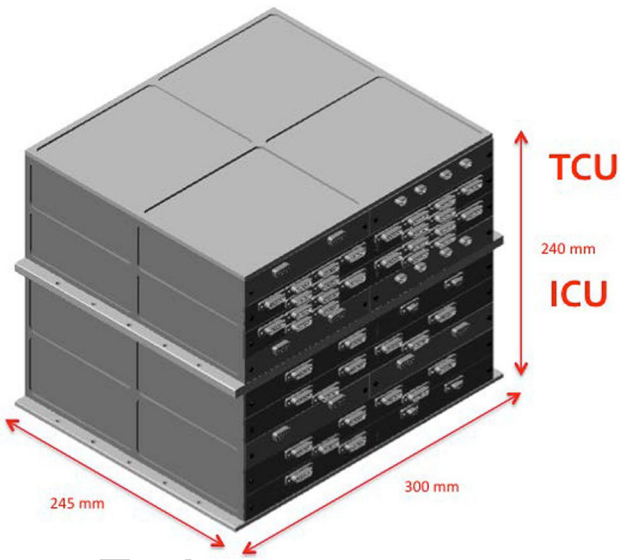

Fig. 16 ARIEL ICU and TCU mechanical design. TCU is considered an ICU slave subsystem

(< 60 K for SIDECARs and < 42 K for detectors), so that both the AIRS CH0 and CH1 are fed and controlled thanks to the adoption of two DCU boards, residing in the warm side of the S/C SVM. The two electronics parts will be connected by means of cryoharnessing, mechanically and thermally interfacing the three V-grooves working at different temperatures.

The active thermal stabilization (± 50 mK, achieved with 10 mK thermistors resolution and a PID controller hosted by TCU) is required only for the detectors of the two AIRS FPAs. The temperature fluctuations of the SIDECARs around their working temperature are not affecting the detectors performance (for the instrument cavity temperature, refer to Fig. 13b). SIDECAR is mainly a digital ASIC and its voltage biases are finely regulated and already filtered in the previous DCU stage, so no meaningful thermal-induced fluctuations and thermal noise are expected on the detectors biases when operating AIRS within the foreseen readout schemes, mainly correlated double sampling/sampling up the ramp, and typical integration times.

The unit adopts a partial cold redundancy and cross-strapping capability. In particular, both TCUs and DCUs are cross-strapped and can work along with PSU and DPU boards (Nominal and Redundant) as a whole, although DCUs are n-t involved in a cold redundant configuration as no duplicated DCUs are foreseen. A very similar ICU architecture, involving DCUs as the SIDECAR I/F (for biases, clock, and control signals), has been already designed and adopted for the Euclid Mission (NISP Instrument [35]). It has been developed by the Italian industry working in strict collaboration with Teledyne to address any SIDECAR I/F and detector management issues. Each DCU controls and interfaces a single SIDECAR (as well as the related detector) in the same configuration adopted for NISP and, in this

Journal : Large 12567 | Article No : 175 | Pages : 20 | MS Code : CEAS-D-17-00051 | Dispatch : 26-10-2017

sense, can be considered for the ARIEL payload a strong heritage from the Euclid project.

Indeed, for the existing design, an overall DPU + DCU + SIDECAR + H1RG detector chain/system reliability figure, higher than 98%, has been computed and for this reason redundancy for ARIEL DCUs, as well as for NISP, has not been considered, also because the related increasing complexity and needed budgets. For the same reasons and to avoid an increased thermal dissipation due to the presence of a multiplexing stage near to the SIDECAR ASICs and FPAs, the AIRS CFEEs' cross-strapping has been excluded from the baseline design.

At the present time, DCU TRL is higher than 5 and a DCU EM model has been already manufactured and fully tested as it is working properly along with the SIDECAR ASIC and the detector. In addition, a DCU EQM model (very similar to the EM one) has been developed and manufactured and is presently under testing (end of tests was initially foreseen by spring 2017). Moreover, a DCU/SIDECAR I/F simulator was developed and adopted by the Euclid Team. The same philosophy concerning simulator is presently foreseen for the ARIEL case [36].

As baseline, all the ICU and TCU boards, both N and R are designed in 6U and 3U formats (233 mm × 160 mm and 160 mm × 100 mm). They are stiffened by a proper mechanical frame with the external I/O connectors fixed and screwed to the board external panels. The lateral sides of the modules are equipped with card-lock retainers, used to fix the modules to the unit internal frame and to facilitate the thermal dissipation towards the base plate. All the box panels are made of an aluminium alloy, and except the bottom panel, they are foreseen to be externally painted in black to improve radiating exchange with the environment and assure a proper thermal conduction towards the SVM bench.

A brief description of the single boards composing the ARIEL ICU is reported in the following sections.

6.1 DPU

The data processing unit board is based on a CPU (the UT699E processor from Cobham Gaisler), a co-processing FPGA, memories for booting (PROM), to host the ASW (E2PROM and/or NVM, e.g., MRAM), for data buffering (SDRAM) and to support data processing (SRAM and SDRAM) as well.

The selected LEON3FT CPU is a SPARC V8 microprocessor running @ 66 MHz or @ 100 MHz, for the E version, allowing up to 140 DMIPS. The processor will run the ASW on the RTEMS OS. One of the main characteristics of the UT699E CPU is the on-board availability of four embedded space wire links (two supporting the RMAP protocol) allowing to be directly interfaced to the SVM and to the DCU SpW I/Fs.

The DPU, as baseline, is in charge of data processing and lossless compression (if needed, e.g., adopting the RICE algorithm, providing a lossless compression ratio CR = 2 at least). It receives 16 bit raw data (pixel raw values) from the SIDECAR ASICs and, once processed (24 bit can be adopted for the ramps slopes, adding 8 bit needed for data quality criteria), it packetizes and send them in CCSDS protocol format towards the S/C CDMS for storing and later downloading to Ground. Pre-processing and compression tasks can be disabled in case of a raw data request from the Spacecraft/Ground.

6.2 DCU

The detector control unit board [33] [36] represents the warm front-end electronics (WFEE) to the cold side of the AIRS spectrometer, i.e., SIDECARs and detectors. It is basically a heritage of the same unit developed and tested for the Euclid Mission [37] and shall host, as baseline, a FLASH-based reprogrammable FPGA to offer maximum flexibility, useful in case of a further update of the processing requirements specification from the ARIEL Science Team during the project lifetime. Alternatively, a one-time-programmable (OTP) FPGA in anti-fuse technology could be adopted, in case no late processing requirements update will be expected.

The baseline selected FPGA is a Microsemi ProASIC3-type device offering the capability to host on-board an hardware description language finite state machine (HDL FSM) with some programmable science data pre-processing tasks (e.g., pixels reordering, data pre-processing etc.) by means of a flexible parameters selection that can be reprogrammed up to the EQM/FM unit. The FPGA also hosts an SDRAM memory controller to manage 128 MB, as baseline, of memory used to support the HDL-based pre-processing tasks.

The DCU WFEE is in charge of the SIDECAR clocking, as at least a master clock is needed for the ASIC, and feeding (secondary finely regulated voltages produced by an on-board Point of Load—PoL), and it collects digitized scientific data and HK (currents, voltages, and temperatures at 12 bit resolution) describing the ASIC and detector status.

The DCU secondary voltages required by SIDECAR shall respect the stability requirements that are basically driven by the detector full well (~ 80e^- assumed) and allowed readout noise (5e^-), along with the contributions coming from the other sources of noise in the overall error budget, to guarantee the required dynamic range within a charge integration. The allowed readout noise can be expressed in terms of voltage fluctuations on the readout amplification stage, i.e., ≤ 62 μV rms or ≤ 62 nV/Hz$^{1/2}$ rms as noise spectral density, so the overall voltage fluctuations on the biases produced by both DCU and SIDECAR shall be compliant with this budget. Given the temperature stability of the instrument

Journal : Large 12567 | Article No : 175 | Pages : 20 | MS Code : CEAS-D-17-00051 | Dispatch : 26-10-2017

cavity, no meaningful voltages variations (Johnson noise) due to thermal fluctuations are expected on the SIDECARs and detectors biases.

6.3 TCU

The telescope control unit is composed of three distinct boards hosted by a different box, as the volume of the electronics to fulfill its design requirements is bigger than a standard 6U board as previously adopted and also to ease AIT/AIV activities at subsystem and payload level, since the units, ICU and TCU, can be operated independently.

The TCU shall be able to accomplish the following metrology tasks [30] in ARIEL Science mode:

- drive the M2 refocusing mechanism;
- drive the IR calibration lamp;
- monitor the thermal state of several PLM elements;

and to address the thermal stabilization requirements derived to guarantee the needed performance, as extrapolated from the Instrument's TMM

- Actively control the thermal stability of the Thermal Control System (TCS) for the following PLM subsystems:
  - AIRS detectors (actively cooled via JT cooler and stabilized; required ± 50 mK achieved with 10 mK thermistors resolution and a PID controller for managing the relative heater on TCS);
  - FGS1/Vis-Phot detector (actively stabilized; required ± 50 mK achieved with 10 mK thermistors resolution and a PID controller for managing the relative heater on TCS);
  - FGS2/NIR-Spec detector (actively stabilized; required ± 50 mK achieved with 10 mK thermistors resolution and a PID controller for managing the relative heater on TCS);
  - M1 mirror (actively stabilized; required ± 1 K achieved with 100 mK thermistors resolution and a PID controller for managing the relative heaters).

A 6U PCB named thermal stabilizer and IR calibrator (TSIRC) will hosts the PLM thermal monitoring and control HW, their multiplexing stages, the IR calibration lamp drivers and an HDL FSM embedded in a FPGA to control the TCU boards as well as to gather and transmit all the generated HK data. For the driver electronics of M2 mechanism, it is foreseen an upgraded version of Euclid's or Gaia's M2M, with the same driver, which will require a separated 6U board for both nominal and redundant systems (M2MD board). To reduce M2MD modifications to fit ARIEL requirements, as well as to reduce the number of interfaces from ICU's PSU, simplifying it, a dedicated 3U board PSU is foreseen (TCU-PSU), which will generate (from the main power line of + 28 V coming from ICU) all the voltage levels required by the M2MD and TSIRC boards.

The system will be based on a cold redundancy, with all boards resting inside a dedicated box on top of ICUs, as represented in Fig. 16.

7 Conclusions

In this paper, the main characteristics of the ARIEL telescope, its thermal control system, and payload control electronics have been presented. An introduction on the mission design and goals has been given together with a description of the various elements composing the spacecraft and payload.

The afocal telescope layout solution has been described and the different requirements and characteristics have been discussed. In particular, the requirements on the FoV of the telescope related to the spectrometer and field guidance channels have been illustrated in detail.

The theoretical performance of the baseline telescope layout, an eccentric pupil Cassegrain plus a collimating off-axis paraboloidal mirror, has been shown and a preliminary study on the passive/active thermal control of the instrument has been given. The telescope is passively cooled at an operating temperature below 70 K.

The instrument control unit baseline electrical architecture, together with that of the telescope control unit, has been described along with the main characteristics of the thermal control system.

Acknowledgements This activity has been realized under the Agenzia Spaziale Italiana (ASI) contract to the Istituto Nazionale di Astrofisica (INAF) (ARIEL 2015-038-R.0). The support from the ESA ARIEL Study Team is gratefully acknowledged.

References

1. Puig, L., Pilbratt, G.L., Heske, A., Escudero Sanz, I., Crouze, P.-E.: ESA M4 mission candidate ARIEL. Proc. SPIE **9904**, 99041W (2016)
2. Tinetti, G., et al.: The science of ARIEL (atmospheric remote-sensing infrared exoplanet large-survey). In: Proceedings of SPIE 9904, 9904, 99041X (2016)
3. Perryman, M., et al.: Astrometric exoplanet detection with Gaia. ApJ **797**(14) (2014)
4. Borucki, W.J., et al.: Kepler planet-detection mission: introduction and first results. Science **327**(5968), 977–980 (2010)
5. Howell, S.B., et al.: The K2 mission: characterization and early results. PASP **126**, 398–408 (2014)

6. ARIEL Science Study Team: ARIEL atmospheric remote-sensing infrared exoplanet large-survey—enabling planetary science across Light-Years, Assessment Study Report (Yellow Book), ESA/SCI(2017)2 (2017)
7. Ricker, G.R., et al.: The transiting exoplanet survey satellite. Proc. SPIE **9904**, 99042B (2016)
8. Fortier, A., et al.: CHEOPS: a space telescope for ultra-high precision photometry of exoplanet transits. Proc. SPIE **9143**, 91432J (2014)
9. Ragazzoni, R., et al.: PLATO: a multiple telescope spacecraft for exo-planets hunting. Proc. SPIE **9904**, 990428 (2016)
10. ARIEL Science Study Team: ARIEL Science Requirements Document, ESA-ARIEL-EST-SCI-RS-001 (2016)
11. ARIEL Science Study Team: ARIEL Mission Requirements Document, ESA-ARIEL-EST-MIS-RS-001 (2016)
12. Papageorgiou, A., et al.: ARIEL performance model, ARIEL-CRDF-PL-ML-001_2.0. https://arielspacemission.files.wordpress.com/2017/05/ariel-crdf-pl-ml-001_performance_model-iss-2-01.pdf (2017)
13. Sarkar, S., et al.: Exploring the potential of the ExoSim simulator for transit spectroscopy noise estimation. Proc. SPIE **9904**, 99043R (2016)
14. Sarkar, S., et al.: ARIEL performance analysis report, ARIEL-CRDF-PL-AN-001_2.2. https://arielspacemission.files.wordpress.com/2017/05/ariel-crdf-pl-an-001-performance-analysis-report-iss-2-2_01.pdf (2017)
15. Sarkar, S., et al.: The effects of stellar variability on transit spectroscopy observation in the ARIEL space mission examined using the ExoSim simulator, EPSC Abstracts 11, EPSC2017-447-2 (2017)
16. Da Deppo, V., et al.: Design of an afocal telescope for the ARIEL mission. Proc. SPIE **9904**, 990434 (2016)
17. Eccleston, P., et al.: An integrated payload design for the atmospheric remote-sensing infrared exoplanet large-survey (ARIEL). Proc. SPIE **9904**, 990433 (2016)
18. Wright, G.S., et al.: The mid-infrared instrument for JWST, II: design and Build. Publ Astron. Soc. Pac. **127**(953), 595–611 (2015)
19. Morgante, G.: Cryogenic characterization of the Planck sorption cooler system flight model. JINST **4**, T12016 (2009)
20. http://www.teledyne-si.com/pdf-imaging/H1RG%20Brochure%20-%20GBA%20&%20Flight%20v2.pdf
21. Eccleston, P.: ARIEL payload design description, ARIEL-RAL-PL-DD-001_2.0. https://arielspacemission.files.wordpress.com/2017/05/ariel-ral-pl-dd-001_ariel-payload-design-description_iss-2-01.pdf (2017)
22. McMurthy, C., et al.: Development of sensitive long-wave infrared detector arrays for passively cooled space missions. Opt Eng **52**(9), 091804-1/-9 (2013)
23. Middleton, K., et al.: ARIEL throughput budget, ARIEL-RAL-PL-TN-005 (2017)
24. Rutten, H., van Venrooij, M.: Telescope optics. Willmann-Bell Inc., Richmond (1999)
25. Sheikh, D.A.: Improved silver mirror coating for ground and space-based astronomy. Proc. SPIE **9912**, 991239 (2016)
26. Philips, A.C., et al.: Progress and new techniques for protected-silver coatings. Proc. SPIE **9151**, 91511B (2014)
27. Schürmann, M.: High-reflective coatings for ground and space based applications. In: Proceedings of the International Conference on Space Optics (ICSO) 2014, Tenerife, Canary Island, Spain, 7–10 October 2014 (2014)
28. Da Deppo, V., et al.: ARIEL telescope material trade-off, ARIEL-INAF-PL-TN-004_2.0. https://arielspacemission.files.wordpress.com/2017/05/ariel-inaf-pl-tn-004_telescope_material_selection_iss-21.pdf (2017)
29. Da Deppo, V., et al.: The afocal telescope optical design and tolerance analysis for the ESA ARIEL mission, OSA technical digest. In: International Optical Design Conference, Denver, Colorado United States, 9–13 July 2017 (2017)
30. Sierra Roig, C., et al.: The ARIEL ESA mission on-board metrology. In: Proceedings of the IEEE International Workshop on Metrology for Aerospace (MetroAeroSpace), Padua, Italy, 21–23 June 2017, pp. 120–125 (2017)
31. De Sio, A., et al.: Alignment procedure for detector integration and characterization of the CaSSIS instrument onboard the TGO mission. Proc. SPIE **9904**, 990452 (2016)
32. D'Ascanio, D., et al: PLM thermal analysis report TMM/GMM description and results, ARIEL-INAF-TN-0003_2.0. https://arielspacemission.files.wordpress.com/2017/05/ariel-inaf-pl-tn-0003_is_2_0_ariel-plm-thermal-analysis-report-51.pdf (2017)
33. Focardi, M., et al.: The ARIEL instrument control unit design for the M4 mission selection review of the ESA's cosmic vision program, to be published in special issue on ARIEL. Exp. Astron. (2017)
34. Guellec, F., et al.: ROIC development at CEA for SWIR detectors: pixel circuit architecture and trade-offs, Proceedings of the International Conference on Space Optics (ICSO) 2014, Tenerife, Canary Island, Spain, 7–10 October 2014 (2014)
35. Maciaszek, T., The Euclid Consortium: Euclid near infrared spectrometer and photometer instrument concept and first test results obtained for different breadboards models at the end of phase C. In: Proceedings of the SPIE 9904, 99040T (2016)
36. Focardi, M., et al.: The atmospheric remote-sensing infrared exoplanets Large-survey (ARIEL) payload electronic subsystems. Proc. SPIE **9904**, 990436 (2016)
37. Corcione, L., et al.: The data processing unit of the NISP instrument of the Euclid mission. Proc. SPIE **9143**, 914331 (2014)

Journal: 12567
Article: 175

Springer
the language of science

Author Query Form

Please ensure you fill out your response to the queries raised below and return this form along with your corrections

Dear Author

During the process of typesetting your article, the following queries have arisen. Please check your typeset proof carefully against the queries listed below and mark the necessary changes either directly on the proof/online grid or in the 'Author's response' area provided below

Query	Details Required	Author's Response
AQ1	Please confirm if the author names are presented accurately and in the correct sequence (given name, middle name/initial, family name). Also, kindly confirm the details in the metadata are correct.	
AQ2	Kindly check and confirm the state in affiliation 7.	
AQ3	Kindly check and confirm whether the affiliations 10, 11 are correctly processed and amend if necessary.	
AQ4	Kindfly provide page range for Ref. [3].	
AQ5	Kindly provide access date for Refs. [12, 20, 28, 32].	